Paleoceanography and Paleoclimatology

AGU ADVANCING EARTH AND SPACE SCIENCE

RESEARCH ARTICLE
10.1029/2022PA004581

Key Points:

- Extreme post-1809 cooling in northwestern North America was centered around the Gulf of Alaska and the southern Yukon
- Spatial temperature patterns in North America post-1809 are consistent with the influence of North Pacific decadal variability

Supporting Information:

Supporting Information may be found in the online version of this article.

Correspondence to:

C. Leland,
cleland@ldeo.columbia.edu

Citation:

Leland, C., D'Arrigo, R., Davi, N., Anchukaitis, K. J., Andreu-Hayles, L., Porter, T. J., et al. (2023). A spatiotemporal assessment of extreme cold in northwestern North America following the unidentified 1809 CE volcanic eruption. *Paleoceanography and Paleoclimatology*, *38*, e2022PA004581. https://doi.org/10.1029/2022PA004581

Received 14 NOV 2022
Accepted 11 APR 2023

Author Contributions:

Conceptualization: C. Leland, R. D'Arrigo
Data curation: L. Andreu-Hayles, T. J. Porter, G. Wiles, R. Wilson, S. Beaulieu, R. Oelkers, E. Reid, T. Nixon
Formal analysis: C. Leland, K. J. Anchukaitis
Funding acquisition: R. D'Arrigo, N. Davi, T. J. Porter
Investigation: C. Leland, R. D'Arrigo, N. Davi, K. J. Anchukaitis
Methodology: C. Leland, K. J. Anchukaitis
Project Administration: R. D'Arrigo, N. Davi, T. J. Porter, T. Galloway, M. Mant

A Spatiotemporal Assessment of Extreme Cold in Northwestern North America Following the Unidentified 1809 CE Volcanic Eruption

C. Leland[1,2], R. D'Arrigo[2], N. Davi[1,2], K. J. Anchukaitis[2,3], L. Andreu-Hayles[2,4,5], T. J. Porter[6], T. Galloway[7], M. Mant[7], G. Wiles[8], R. Wilson[2,9], S. Beaulieu[6], R. Oelkers[2], B. V. Gaglioti[2,10], M. P. Rao[2,4,11,12], E. Reid[9], and T. Nixon[2]

[1]Department of Environmental Science, William Paterson University, Wayne, NJ, USA, [2]Tree Ring Laboratory, Lamont-Doherty Earth Observatory of Columbia University, Palisades, NY, USA, [3]Laboratory of Tree-Ring Research, School of Geography, Development, and Environment, University of Arizona, Tucson, AZ, USA, [4]CREAF, Barcelona, Spain, [5]ICREA, Barcelona, Spain, [6]Department of Geography, Geomatics and Environment, University of Toronto Mississauga, Mississauga, ON, Canada, [7]Department of Anthropology, University of Toronto Mississauga, Mississauga, ON, Canada, [8]The College of Wooster, Wooster, OH, USA, [9]School of Earth and Environmental Sciences, University of St Andrews, St Andrews, UK, [10]Water and Environmental Research Center, Institute of Northern Engineering, University of Alaska, Fairbanks, AK, USA, [11]Cooperative Programs for the Advancement of Earth System Science, University Corporation for Atmospheric Research, Boulder, CO, USA, [12]Department of Plant Sciences, University of California, Davis, CA, USA

Abstract Two large volcanic eruptions contributed to extreme cold temperatures during the early 1800s, one of the coldest phases of the Little Ice Age. While impacts from the massive 1815 Tambora eruption in Indonesia are relatively well-documented, much less is known regarding an unidentified volcanic event around 1809. Here, we describe the spatial extent, duration, and magnitude of cold conditions following this eruption in northwestern North America using a high-resolution network of tree-ring records that capture past warm-season temperature variability. Extreme and persistent cold temperatures were centered around the Gulf of Alaska, the adjacent Wrangell-St Elias Mountains, and the southern Yukon, while cold anomalies diminished with distance from this core region. This distinct spatial pattern of temperature anomalies suggests that a weak Aleutian Low and conditions similar to a negative phase of the Pacific Decadal Oscillation could have contributed to regional cold extremes after the 1809 eruption.

1. Introduction

The early nineteenth century was one of the coldest periods of the Little Ice Age (LIA; ~1450–1850; Grove, 1988; PAGES 2k Consortium, 2019; Wilson et al., 2016a). Cold conditions during this time have been attributed to several large tropical volcanic eruptions, as well as reduced solar activity during the Dalton Minimum (~1790–1830 CE; Brönnimann et al., 2019). The most significant eruption of this period, the 1815 Tambora event in Sumbawa, Indonesia, resulted in the largest volcanic stratospheric sulfur injection (VSSI) of the nineteenth century, with well-documented but varying regional climatic and human impacts during the subsequent "year without a summer" of 1816 (Brönnimann & Krämer, 2016; D'Arrigo et al., 2013; Harington, 1992; Oppenheimer, 2003; Raible et al., 2016). The second largest volcanic event during the nineteenth century and the twelfth largest eruption of the past 2,500 years in terms of estimated VSSI was the "unidentified" eruption of 1808 or 1809 (Timmreck et al., 2021; Toohey & Sigl, 2017). Although relatively little is known about this eruption, including its specific location and timing, it was clearly a significant event with the potential to impact climate on a global scale.

Evidence of a major volcanic event in 1808 or 1809 was first identified in ice core records from Antarctica and Greenland (Cole-Dai et al., 2009; Dai et al., 1991). The simultaneous sulfate peak in ice cores from both poles suggests that a tropical eruption likely occurred in ~February 1809 (±4 months), and an associated sulfur isotope anomaly is consistent with a large stratospheric eruption (Cole-Dai et al., 2009). While there are no direct observations of an eruption at this time, a stratospheric aerosol veil was reported by meteorologists in both Colombia and Peru, indicating that a tropical Pacific eruption might have occurred late in 1808 (Guevara-Murua et al., 2014). Chenoweth (2001) noted a sudden cooling in historical Malaysian air temperature records, suggesting an earlier eruption date of March-June 1808. Regardless of the exact timing, this unidentified volcanic event

Resources: R. D'Arrigo, N. Davi, K. J. Anchukaitis, G. Wiles, R. Wilson, S. Beaulieu, R. Oelkers, B. V. Gaglioti, M. P. Rao
Supervision: R. D'Arrigo, N. Davi, L. Andreu-Hayles
Visualization: C. Leland, K. J. Anchukaitis
Writing – original draft: C. Leland
Writing – review & editing: R. D'Arrigo, N. Davi, K. J. Anchukaitis, L. Andreu-Hayles, T. J. Porter, T. Galloway, M. Mant, G. Wiles, R. Wilson, S. Beaulieu, R. Oelkers, B. V. Gaglioti, M. P. Rao, E. Reid, T. Nixon

is associated with cold tropical Pacific sea surface temperatures (SSTs), which were sustained for several years (D'Arrigo et al., 2006, 2009; Tierney et al., 2015). In addition to a potential tropical eruption, an 1809 tephra layer in a Yukon ice core suggests that a high-latitude Northern Hemisphere volcanic eruption may have occurred around the same time (Yalcin et al., 2006). Thus, while the specific location(s) and timing of the volcano(es) remains unknown, herein we refer to this general event as the 1809 volcanic eruption.

After the 1809 volcanic event, there is evidence of cooling in Northern Hemisphere tree-ring based temperature reconstructions, and temperatures generally remained low up to the cooling associated with the Tambora eruption (Büntgen et al., 2021; Schneider et al., 2015, 2017; Stoffel et al., 2015; Timmreck et al., 2021; Wilson et al., 2016a). While cooling occurred in the Northern Hemisphere on average, climate field reconstructions from Anchukaitis et al. (2017) show a distinct and highly heterogenous spatial pattern of post-1809 summer temperature anomalies in some northern regions, particularly in North America (Timmreck et al., 2021). Paleoclimatic studies in northwestern North America (NWNA) report extreme and sometimes record-breaking cold conditions in years directly following 1809 and preceding the Tambora eruption (Appleton & St. George, 2018; Briffa et al., 1994; Davi et al., 2003a; Edge et al., 2021; Wiles et al., 2014; Wilson et al., 2019a). By contrast, relatively mild temperatures are reconstructed for parts of eastern Canada during this period (Anchukaitis et al., 2017; Timmreck et al., 2021).

The mechanisms responsible for the particularly cold temperatures over much of NWNA following the 1809 eruption, and the prominent zonal temperature dipole across North America, remain to be further explored. It is well-established that large, explosive eruptions can significantly impact interannual as well as decadal climate variability via both radiative effects and dynamic responses of the ocean-atmosphere system (Robock, 2000; Zanchettin, 2017). In NWNA, Vargo (2013) hypothesized that the 1809 eruption could have intensified a negative phase of the Pacific Decadal Oscillation (PDO; e.g., Wang et al., 2012), exacerbating the extreme cold conditions that were reconstructed around the Gulf of Alaska (GOA). The PDO, the leading statistical mode of SST variability in the North Pacific (Mantua et al., 1997; Newman et al., 2016), is associated with temperature and precipitation anomalies around the Pacific Basin and beyond, including North America (e.g., McAfee, 2014; McCabe et al., 2004; Mills & Walsh, 2013). The negative phase of the PDO is characterized by cool SSTs along the northeast Pacific coast, and generally cooler surface air temperatures around the GOA and adjacent regions, particularly in winter and spring (S. W. Fleming & Whitfield, 2010). Some climate modeling experiments suggest that strong tropical volcanism might dynamically force a negative phase of the PDO (Fang et al., 2022; Wang et al., 2012). In contrast, other studies do not show a consistent forced response of the PDO/North Pacific variability to volcanism, suggesting that internal variability and/or pre-existing ocean conditions play an important role (L. E. Fleming & Anchukaitis, 2016; Zanchettin, Rubino, et al., 2013). If volcanism can initiate or enhance a negative phase of the PDO, however, this would have important implications for broad-scale temperatures and hydroclimate, as well as ecosystem processes, with notable impacts on marine fisheries (Mantua et al., 1997), and marine mammal and seabird populations (Anderson & Piatt, 1999).

The PDO is the Northern Hemisphere manifestation of a combination of several interacting ocean-atmosphere phenomena, including the Aleutian Low, El-Niño Southern Oscillation (ENSO), the Kuroshio Extension (KOE), and ocean memory (Newman et al., 2016). Tree-ring-based PDO reconstructions do not agree well prior to the observational period, likely reflecting the complexity and instability of the PDO and its regional teleconnections, as well as geographic and seasonal biases in tree-ring data (Newman et al., 2016; St. George, 2014; Wise, 2015). Nevertheless, the initial background conditions of the climate system, including internal climate variability (such as the PDO) and external forcings, can be important in the evolution of climate following major volcanic eruptions (e.g., Illing et al., 2018; Lough & Fritts, 1987; Zanchettin, 2017; Zanchettin, Bothe, et al., 2013; Zanchettin, Rubino, et al., 2013). Assessing large-scale temperature patterns in the early nineteenth century could help clarify whether North Pacific decadal variability was associated with the distinct spatial climate anomalies observed after the 1809 eruption.

Given the extant uncertainties associated with the unidentified eruption of 1809 and its regional climate impacts across NWNA, here we describe and quantify the magnitude and duration of cold temperatures after the 1809 event across the region using a high-density network of previously developed temperature-sensitive tree-ring records, including eight temperature reconstructions and two temperature-sensitive chronologies. We further explore the potential association between North Pacific decadal variability and the 1809 cooling event via detailed analysis of the NWNA tree-ring records, as well as existing larger-scale spatial climate reconstructions.

10.1029/2022PA004581

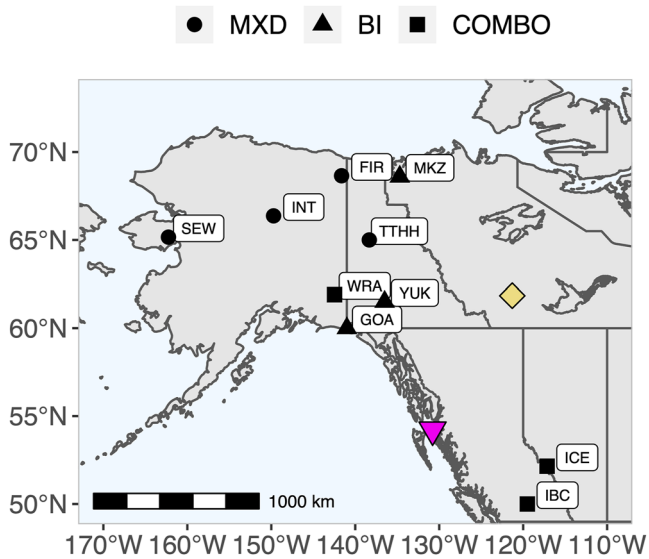

Figure 1. A map of published tree-ring temperature records used for analysis of climate after the 1809 eruption across northwestern North America (NWNA). The symbols represent the parameter(s) used in each regional reconstruction or record of past temperature (circle: maximum latewood density (MXD); triangle: blue intensity (BI); square: combination of multiple parameters (BI, MXD and/or ring width)). The tree-ring reconstructions (Table 1) are derived from chronologies from multiple sites, and the legend point represents the central area of those sites. More information on the individual temperature reconstructions and records can be found in Table 1. The yellow diamond represents the mouth of the Liard River in the Northwest Territories, where a historical record indicates cold conditions during the winter of 1810–1811 (see Discussion). The magenta upside down triangle represents the location of the Edge et al. (2021) bivalve reconstruction (see Discussion).

2. Methods

2.1. NWNA Tree-Ring Data Network

To evaluate temperature variability following the 1809 eruption across NWNA, we compiled a network of ten tree-ring temperature reconstructions and temperature-sensitive chronologies from Alaska (USA), and from western Canada: the Yukon, Northwest Territories, British Columbia, and Alberta (Figure 1). We used records already analyzed in the scientific literature (see Table 1 for details). Seven of these records are published regional spring/summer temperature reconstructions that were produced from multiple site chronologies and parameters. Details on the Mackenzie Delta (MKZ) minimum temperature reconstruction, recently described by Beaulieu (2022), are provided in Text S1 of Supporting Information S1. Two records, Firth (FIR) and Twisted Tree-Heartrot Hill (TTHH), are individual temperature-sensitive chronologies. FIR was previously used to reconstruct past summer temperatures in Anchukaitis et al. (2013b), but a calibration method was employed to preserve lower frequency (multidecadal and longer) variability at the expense of the high frequency (interannual) signal. Here we use the Firth maximum latewood density (MXD) chronology from Anchukaitis et al. (2013b), which allows us to analyze the higher frequency variability associated with a single volcanic eruption. Tree-ring data from TTHH was previously used to assess temperatures and post-volcanic cooling from northern treeline sites (ring-width in Jacoby and Cook (1981); MXD in D'Arrigo and Jacoby (1999)), though here we use and update the MXD record by applying age-dependent spline detrending (Melvin et al., 2007) using a signal-free framework with the RCSsigFree software (E. R. Cook & Krusic, 2020) to reduce potential trend distortion (Melvin & Briffa, 2008). Spatial correlations between the TTHH record and maximum July–August temperatures (CRUTS4.05; Harris et al., 2020) demonstrate the sensitivity of the MXD parameter to late summer temperatures (Figure S1 in Supporting Information S1).

These ten tree-ring records were selected to maximize the contribution of MXD and Blue Intensity (BI) data sets. MXD and BI are considered superior

Table 1
Warm-Season Reconstructions and Tree-Ring Chronologies From NWNA

Region	Code	Publication	Time span	Climate/Reconstruction variable (season; $_aR^2$)	Parameters
Interior British Columbia	IBC	Wilson et al. (2014)	1600–1995	T_{max} (MJJA; 0.52–0.55[a])	RW, MXD, BI
Icefields	ICE	Luckman and Wilson (2005b)	950–1994	T_{max} (MJJA; 0.53)	RW, MXD
Gulf of Alaska	GOA	Wilson et al. (2017)	1600–2010	T_{mean} (JJAS; 0.38)	BI
Southern Yukon	YUK	Wilson et al. (2019a)	1337–2004	T_{max} (MJJA; 0.46)	BI
Wrangell Mountains	WRA	Davi et al. (2003a)	1593–1992	T_{mean} (JAS; 0.51)	MXD
Twisted Tree-Heartrot Hill	TTHH	D'Arrigo and Jacoby (1999)	1530–1992	T_{max} (JA; **)	MXD
Seward Peninsula	SEW	D'Arrigo et al. (2004)	1389–2001	T_{mean} (MJJA; 0.38)	MXD
Interior Alaska	INT	Jacoby et al. (1999)	1680–1990	T_{mean} (MJJA; 0.41)	MXD
Mackenzie Delta	MKZ	Beaulieu (2022)	1105–2017	T_{min} (MJJAS; 0.40)	BI
Firth River	FIR	Anchukaitis et al. (2013b)	1073–2004	T_{mean} (JA; 0.36[b])	MXD

Note. T_{max}, T_{mean}, and T_{min} refer to maximum, mean, and minimum temperatures, respectively. The adjusted R^2 ($_aR^2$) reported in each publication for the calibration period is shown (the full calibration period, spanning both the initial calibration and validation time periods, are provided when available). ** The TTHH MXD chronology has not been used for climate reconstruction, but regional correlations with T_{max} are shown in Figure S1 of Supporting Information S1.
[a]Range of $_aR^2$ values from five temperature reconstruction variants combined using a weighted mean in Wilson et al. (2014). [b]Mean of calibration and validation R^2 from an ensemble of reconstructions.

for tracking post-volcanic cooling responses, in contrast to ring width, which typically show a muted or lagged response (Anchukaitis & Smerdon, 2022; Anchukaitis et al., 2012; D'Arrigo et al., 2013; Esper et al., 2015; Fuentes et al., 2018; Lücke et al., 2019; Reid & Wilson, 2020). While most of the records used here are based entirely on MXD or BI data sets, two of the reconstructions, Interior British Columbia (IBC; Wilson et al., 2014) and Icefields (ICE; Luckman & Wilson, 2005b), also incorporated ring-width data. Both reconstructions however explain more than 50% of the local summer temperature variance (Table 1) and track the persistence properties of the instrumental data very well (Luckman & Wilson, 2005b; Wilson et al., 2014). Although the target variables of the temperature reconstructions differ (i.e., we use a combination of maximum, mean, and minimum temperature targets; Table 1), the reconstructions similarly capture relative changes in warm-season temperatures over the last several centuries and are useful for assessing short-term temperature changes after volcanic eruptions.

2.2. Spatial Assessment of Post-1809 Temperatures

The top-10 coldest individual years and the top-three coldest non-overlapping decades over the common period (1680–1990) were ranked for each normalized ($\mu = 0$, $\sigma = 1$) record to determine whether there was evidence of extreme cooling following the 1809 eruption. We also specifically compared temperatures among sites during 1810 and the 1809–1814 (6-year) period, just preceding the eruption of Mount Tambora in April of 1815. These time windows were selected because an initial volcanic cooling in 1809 in Northern Hemisphere temperatures has been reported and temperatures remained below average until at least the Tambora eruption (Schneider et al., 2017; Timmreck et al., 2021).

To quantify both the degree and persistence of cooling for each record from 1809 to 1814, we calculated a "cold severity index." First, all records were normalized ($\mu = 0$, $\sigma = 1$) over the 1680–1990 common period. Then, cold severity (CS) was calculated over running 6-year periods (P) for each record as follows:

$$\mathrm{CS}_P = M_P * N_P$$

where M_P refers to the magnitude, or the average normalized temperature, and N_P refers to the number of years with a below average normalized temperature, for each 6-year period. This formulation is similar to a runs analysis (e.g., Dracup et al., 1980), though here, a 6-year moving window is pre-defined and consecutive below-average temperatures are not required. This formulation allows the comparison of the 1809–1814 period against all other available 6-year periods while considering both average temperatures and the duration of cooling. We also calculated cold severity using shorter temporal windows for comparison (1809–1811, 1809–1812, and 1809–1813).

2.3. North Pacific Decadal Variability and Post-1809 Temperatures

We investigated potential connections between North Pacific decadal variability and temperature anomalies after the 1809 eruption across both the NWNA tree-ring network and more broadly across northern North America (including eastern Canada). Here, North Pacific decadal variability is assessed in terms of the PDO index and the North Pacific Index (NPI, a measure of variability in the Aleutian Low). The PDO is the leading mode of an empirical orthogonal function (EOF) of monthly averaged SST anomalies from the North Pacific (20°–70°N) after removing global mean SSTs (Mantua et al., 1997; Newman et al., 2016), and the NPI measures sea level pressure averaged over 30°–65°N and 160°–140°E. We used the Mantua PDO index from the Joint Institute for the Study of the Atmosphere and Ocean (JISAO; http://research.jisao.washington.edu/pdo/PDO.latest.txt), and the Trenberth and Hurrell North Pacific Index from the National Center of Atmospheric Research (NCAR; Trenberth & Hurrell, 1994).

To test whether the spatial signature of the post-1809 temperature response across NWNA was associated with North Pacific decadal variability, we compared the 1809–1814 cold severity index of each record with the observed correlation between each record and the PDO and NPI indices over the twentieth century. Correlations between each tree-ring record and instrumental measures of North Pacific climate variability were computed from 1900 to 1990, as 1990 is the final common year of all records. We used annual, cold season (October–March), and warm season (April-September) averages of PDO/NPI indices for correlation analysis. The relationship between 1809–1814 cold severity and measures of PDO/NPI correlations across all records was quantified with a linear regression. We also compared the 1809–1814 cold severity of each record against the degree of temperature difference between a warm (1977–1984) and cool (1968–1975) phase surrounding the well-documented ~1976

PDO regime shift (Ebbesmeyer et al., 1991). This temperature difference is herein referred to as the Δ regime shift, in which the average cool phase (1968–1975) temperature was subtracted from the average warm phase (1977–1984) temperature for each reconstruction. All analyses were repeated after detrending the records from 1900 to 1990 to remove the potential influence of long-term trends on results.

Next, we evaluated the spatial characteristics of the post-1809 temperature response across northern North America using the ensemble mean of the Northern Hemisphere Tree-ring Network Development-data assimilation (NTREND-DA) temperature reconstructions (King et al., 2021a). This paleo data set was produced through data assimilation methods using the NTREND network of tree-ring chronologies (Anchukaitis et al., 2017; Wilson, Anchukaitis, et al., 2016a) to reconstruct May-August temperature anomalies across the Northern Hemisphere (King et al., 2021a). Although the NTREND proxy network is composed of many of the tree-ring records from NWNA analyzed here, the NTREND-DA product allows for a broader-scale assessment of patterns of temperature anomalies across North America. Spatial patterns of the reconstructed temperature response post-1809 were compared with teleconnection patterns between temperatures and PDO/NPI indices across North America during the observational period. We correlated surface air temperatures from National Centers for Environmental Prediction—National Center for Atmospheric Research (NCEP/NCAR) reanalysis data with annual, winter, and summer mean PDO/NPI indices from 1948 to 2020.

We assessed potential PDO variability in the late eighteenth and early nineteenth centuries, specifically around the 1809 eruption, through comparisons with several proxy-reconstructed records. Five tree-ring based PDO reconstructions were evaluated from the literature (Biondi et al., 2001; D'Arrigo & Wilson, 2006b; D'Arrigo et al., 2001; Gedalof & Smith, 2001; MacDonald & Case, 2005b), with another PDO series derived from the leading mode of a Pacific SST tree-ring based reconstruction (Evans et al., 2001) over the North Pacific domain of 20°–62.5°N and 110°E−110°W. The state of ENSO, a key ocean-atmosphere climate pattern in the tropical Pacific, is also important to consider as it has wide-ranging impacts on climate, including the North Pacific and northwestern North America particularly during the boreal winter (S. W. Fleming & Whitfield, 2010; Papineau, 2001). We therefore also assessed ENSO variability as estimated from an existing tree-ring based Niño3.4 reconstruction (Li et al., 2013a). Finally, spatial hydroclimate variability from 1809 to 1810 was evaluated from three gridded reconstructions developed from tree-ring networks: the North American Drought Atlas - NADA (E. R. Cook, Seager, et al., 2010); the Monsoon Asia Drought Atlas—MADA (E. R. Cook, Anchukaitis, et al., 2010a); and the Old World Drought Atlas - OWDA (E. R. Cook, Seager, Heim, et al., 2015; E. R. Cook, Seager, Kushnir, et al., 2015). This analysis was conducted to assess whether hemispheric spatial drought patterns could provide further insight on ocean-atmosphere processes around the 1809 eruption. It is important to note that several of the tree-ring based reconstructions described here share the same paleoclimate proxy data, so the comparisons are complementary as opposed to being completely independent.

3. Results and Discussion

3.1. Spatial Temperature Patterns Following the 1809 Eruption

There is a varying temperature signature across the NWNA tree-ring network in the years following 1809 (Figure 2a, Figure S2 in Supporting Information S1, Table 2). The Gulf of Alaska (GOA), Wrangell-St. Elias (WRA), and Southern Yukon (YUK) temperature reconstructions, highlighted in Figure 2, showed the most prominent cooling in the year 1810 (Figures 2 and 3a; Figure S2 in Supporting Information S1). This year was the coldest in the WRA record and ranked as the second and eighth coldest years in the YUK and GOA record, respectively, during the 1680–1990 common period (Table 2). The anomalous cold conditions during 1810 are in agreement with an earlier analysis of MXD records in southern Alaska/Yukon, which was part of a broader compilation for northern North America (Briffa et al., 1994). The year 1809 was also relatively cool in southeastern Alaska/the southern Yukon and is ranked as the fifth coldest year in the WRA record (Figure 2, Table 2). Other years that ranked as extreme cold events soon after the 1809 eruption included 1813 (FIR, IBC, ICE), 1814 (SEW), and 1815 (FIR, YUK, TTHH). As shown by other studies of past temperature variability in NWNA (Briffa et al., 1994; D'Arrigo & Jacoby, 1999), there is no evidence of anomalous cold conditions in 1816 (the "year without a summer") in this region of NWNA. Conversely, cooling following the eruption of Laki (Iceland) in 1783 has been well-documented across the northern/Arctic region of NWNA (e.g., Anchukaitis et al., 2013b; Edwards et al., 2021; Jacoby et al., 1999) and was a top-10 cold event in five records from central/northern Alaska and the Yukon analyzed here (WRA, INT, FIR, SEW, TTHH; Table 2).

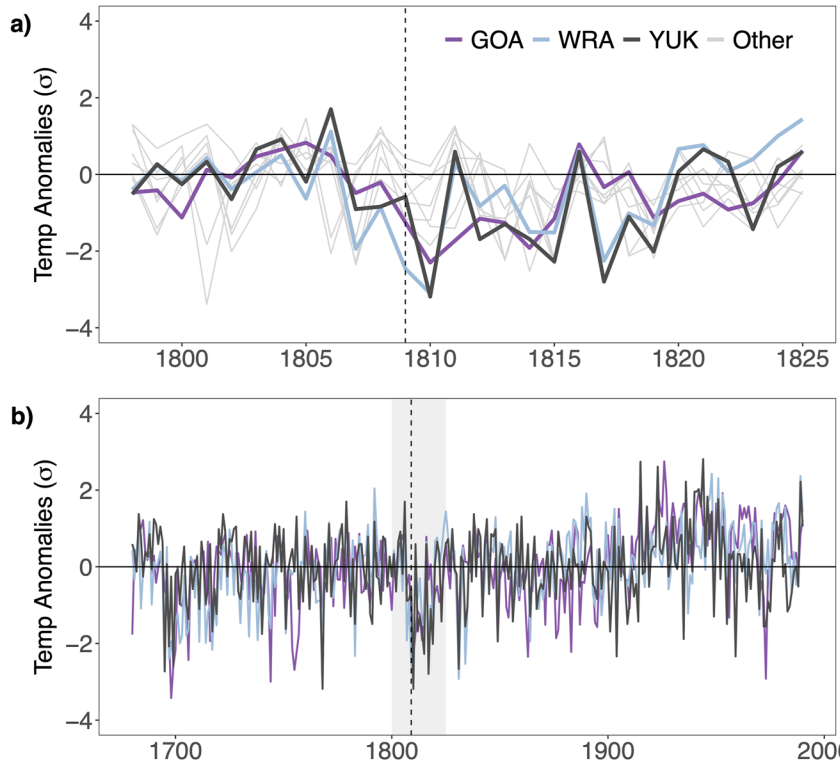

Figure 2. Temperature anomalies for NWNA tree-ring records expressed as z-scores relative to the 1680–1990 common period. The temperature anomalies in the early nineteenth century across all tree-ring records (a) and the 1680–1990 common period from three records (Gulf of Alaska—GOA, purple; Wrangell-St. Elias—WRA, light blue; Southern Yukon—YUK, black) (b) are illustrated and the year 1809 is denoted with a dashed line. The gray box in panel (b) corresponds to the period shown in panel (a). The GOA, WRA, and YUK records, highlighted in both panels, showed the most pronounced cooling after the 1809 eruption.

Table 2
Extreme Cold Years and Decades Across Ten Regions in NWNA

Rank	GOA	WRA	INT	FIR	SEW	IBC	ICE	YUK	TTHH	MKZ
Coldest Individual Years										
1	1698	**1810**	1783*	1783*	1896	1801	1699	1768	1959	1959
2	1744	1831	1695	1699	1783*	1899	1701	**1810**	1699	1870
3	1973	1695	1765	1695	1861	1964	1738	1817	1711	1871
4	1755	1834	1834	1690	1890	1881	1688	1695	1695	1884
5	1699	**1809**	1868	1969	**1814**	1762	1838	1831	1717	1969
6	1706	1697	1864	1959	1834	1876	**1813**	1699	1831	1924
7	1863	1699	1856	**1815**	1766	1880	1833	1904	1783*	1690
8	**1810**	1783*	1807	1685	1856	**1813**	1899	1959	**1815**	1985
9	1756	1817	1861	1791	1864	1959	1696	**1815**	1689	1699
10	1883	1717	1711	**1813**	1695	1976	1731	1697	1819	1980
Coldest Non-overlapping Decades										
1	1697–1706	1697–1706	1827–1836	1783–1792	1855–1864	**1810–1819**	1694–1703	**1810–1819**	1693–1702	1980–1989
2	1751–1760	**1809–1818**	1861–1870	1693–1702	1733–1742	1875–1884	**1818–1827**	1695–1704	**1812–1821**	1884–1893
3	**1806–1815**	1711–1720	1782–1791	**1812–1821**	1762–1771	1780–1789	1829–1838	1904–1913	1711–1720	1969–1978

Note. The top 10 coldest individual years and top three coldest (non-overlapping) decades across the 10 tree-ring records over the common period (1680–1990). The bolded years are those within a decade of the 1809 unidentified eruption. The * indicates an extreme cold year coincident with the 1783 Laki volcanic eruption.

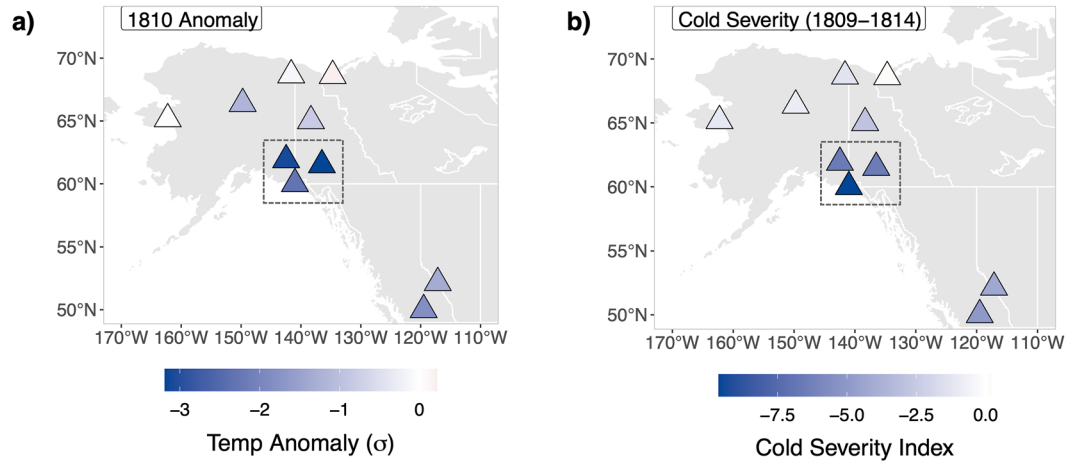

Figure 3. The spatial signature of cold temperatures across NWNA after the 1809 eruption. For each record, we show the 1810 temperature anomaly, expressed as *z*-scores relative to 1680–1990 (a) and the cold severity index (b), calculated as the magnitude of cooling multiplied by the number of years with a below average temperature from 1809 to 1814. The dashed box represents the three records (GOA, WRA, YUK) with the most pronounced cooling signature after the 1809 eruption.

Our index of cold severity, incorporating both the average temperature anomalies and the duration of below-average temperatures from 1809 to 1814, indicates that the most severe conditions occurred in the GOA, WRA, and YUK reconstructions (Figure 3b and Figure S3 in Supporting Information S1). The GOA had the lowest average temperature anomaly from 1809 to 1814 relative to other records in the network and was the only record to sustain below-average temperatures over the entire 6-year window (Figure S3 in Supporting Information S1). WRA and YUK had the next-lowest average temperature anomalies following GOA, and both records showed five years of below-average temperatures over the 1809–1814 period (Figure S3 in Supporting Information S1). The combination of extreme 1810 temperature anomalies and persistent cold severity from 1809 to 1814 (Figure 3) suggests that the GOA and neighboring areas (southeastern Alaska and the southern Yukon) experienced the most immediate and extreme cold conditions in NWNA. The magnitude of cooling weakens in all directions away from the GOA, but particularly toward far northern Alaska (US) and the northern Northwest Territories, Canada (Figure 3). When testing cold severity calculations using different temporal windows (1809–1811, 1809–1812, 1809–1813), the same spatial pattern emerged (Figure S4 in Supporting Information S1). Stine and Huybers (2014) suggested that explosive volcanic eruptions can further decrease tree-ring density measurements via a reduction in light availability, especially in "light-limited" Arctic regions. However, the spatial pattern of cooling anomalies identified here does not correspond well with the pattern of cloudy/clear conditions across NWNA shown in Stine and Huybers (2014), based on sites from the Schweingruber MXD network (Schweingruber & Briffa, 1996). In this study, the southern Yukon, relatively clear-skied in comparison to the Gulf of Alaska, also showed a significant post-1809 cooling response. This suggests that temperature, rather than light limitation, is likely the dominant post-volcanic signal captured in this study.

In support of regional post-volcanic cooling, independent historical information from a report from a Northwest Company clerk in the southern Northwest Territories (Figure 1, yellow diamond), detailed an extremely cold and harsh winter in 1810–1811 with catastrophic impacts, including the starvation and death of many Indigenous peoples and fur traders, thick ice, scarce animals, and a significant loss in trade (Krech, 1978a, 1978b). While this historical account is based on winter conditions and the referenced location is distant from the NWNA sites analyzed here, it is possible that this reported cold event was related to impacts from the 1809 eruption. In the southern and central Yukon, oral histories from Indigenous elders also suggest periods of extreme cold and human loss during the late Little Ice Age, though the exact years are unknown (Cruikshank, 2001, 2007). Further research of historical records and Indigenous oral tradition in NWNA could be a valuable complement or supplement to paleoclimate data for assessing regional climate extremes of the past and potential human-environment interactions (e.g., Adamson, 2015; E. R. Cook, Anchukaitis, et al., 2010a, 2010b; Degroot et al., 2021; Di Cosmo et al., 2018; Jacoby et al., 1999; Liang et al., 2006; Nash et al., 2021; Stahle & Dean, 2011; Woodhouse et al., 2002), particularly with regard to volcanic eruptions (e.g., Blong, 1982; D'Arrigo et al., 2020; Guillet et al., 2017; Mackay et al., 2022; Moodie et al., 1992).

While the years directly following the 1809 eruption were extremely cold in GOA, WRA, and YUK, these records also showed below-average temperatures in the two years preceding the 1809 eruption (Figure 2a), indicating cold background conditions prior to the volcanic event. The cold anomalies in the early 1800s contrasted markedly with warmer conditions in previous decades in this region (Figure 2b). The early 1800s, in general, were cold across much of NWNA, similar to global average trends (Brönnimann et al., 2019; Crowley et al., 2014). Seven of the 10 NWNA records (IBC, ICE, GOA, YUK, WRA, TTHH, FIR) reveal a top-ranked cold decade within the first two decades of the 1800s (Table 2).

3.2. Other Paleoclimate Records of Post-1809 Temperatures in North America

Beyond the tree-ring network described here, there is other paleoclimatic evidence of extremely cold temperatures around NWNA following 1809. An annually resolved bivalve (geoduck) reconstruction of April-September Northeast Pacific SSTs along the coast of British Columbia (Figure 1) showed the coldest decade around 1810 (Edge et al., 2021). The years 1809–1811 were the three coldest years, and 1810 was the single coldest year over the length of the reconstruction, which covers 1725–2008 continuously and includes older radiocarbon-dated segments (Edge et al., 2021). The "year without a summer" (1816) in the bivalve-based reconstruction is also relatively warm, in agreement with tree-ring records from NWNA. In southwestern Alaska, a sub-centennial temperature reconstruction derived from beetles (Coleoptera) suggested that the coldest period in that region, extending back to the mid-fifteenth century, was centered around 1815 CE (Forbes et al., 2020). While this reconstruction is not annually resolved, the record captures the extreme cold of the early 1800s in southern Alaska.

Severe cold following the 1809 eruption has also been reported in tree-ring studies from elsewhere in North America, beyond the NWNA network analyzed here. In the far western United States, for example, tree-ring width and anatomical anomalies from mountain hemlock (*Tsuga mertensiana*) trees in Oregon suggest that the winter of 1809–1810 was remarkably snowy and cold, and unprecedented over almost 500 years (Appleton & St. George, 2018). The year 1810 was also reported as one of the coldest years since 1600 in regions of British Columbia/the Pacific Northwest and California (Briffa et al., 1992). A new temperature reconstruction from yellow-cedar (*Callitropsis nootkatensis*) tree-ring widths in the Cascade Mountains in Washington State (USA) similarly showed 1810 as the coldest year back to at least the fourteenth century (Trinies et al., 2022), whereas 1816 was again unremarkable. Top-ranking multi-year cold events surrounding 1809 were also described in regions of the Rocky Mountains of the western United States based on latewood blue intensity measurements from Englemann spruce (Heeter et al., 2021). A bristlecone pine record comprised of sites in California, Nevada, and Arizona showed frost rings in both 1809 and 1810 (Salzer & Hughes, 2007), providing further evidence of abrupt cold temperatures across relatively lower latitudes in western North America potentially associated with this volcanic eruption.

As previously described by Timmreck et al. (2021), a geographically extensive cooling signature across NWNA is also apparent in gridded spatial reconstructions of warm-season temperatures derived from a Northern Hemisphere tree-ring network (Figure 4 showing the King et al. (2021a, 2021b) data set, with anomalies relative to the 1951–1980 CE mean; also seen in Figure S5 of Supporting Information S1 comparison with Anchukaitis et al. (2017)). There are generally cooler temperatures in the western domain of northern North America, in contrast to average or mildly warm temperatures in the eastern domain from 1809 to 1814 (Figure 4). In agreement with our analysis above, and also reported in Briffa et al. (1994), the most extreme cooling is focused around the southeastern Alaska/southern Yukon region in the year 1810. The prominent east-west temperature dipole pattern across North America occurs during the year 1810, as was also noted earlier in Timmreck et al. (2021), and we found that this dipole weakens from 1811 onwards (Figure 4).

3.3. Post-1809 Cooling in North America and Sensitivity to North Pacific Decadal Variability

Across NWNA, the degree of cold severity from 1809 to 1814 is associated with the correlation between each temperature record and the PDO (cold severity vs. annual PDO correlations (1900–1990): $r = -0.86$, $p < 0.01$; Figure 5a), and the NPI (cold severity vs. annual NPI correlations (1900–1990): $r = 0.89$, $p < 0.01$; Figure 5b). For example, temperatures in the Gulf of Alaska region, which had the most extreme cold severity from 1809 to 1814 (Figure 3b), also show the highest positive correlation with the PDO (Figure 5a) and strongest negative correlation with the NPI (Figure 5b). Conversely, temperatures in the Mackenzie Delta region in the northern

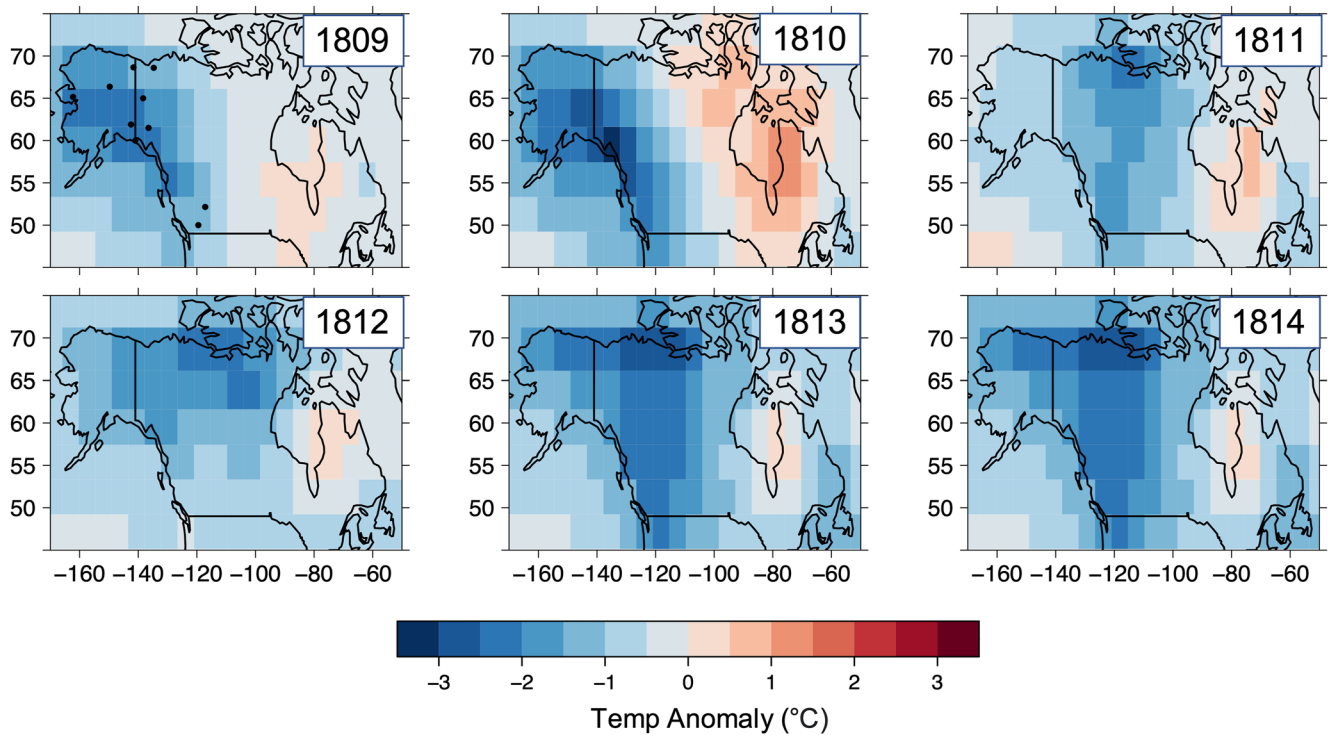

Figure 4. Temperature anomalies across northern North America following the 1809 eruption. These maps show a spatial reconstruction (King et al., 2021a, 2021b) of warm-season (May–August) temperature anomalies (relative to the 1951–1980 CE mean) across northern North America from 1809 to 1814. The dots in the 1809 panel show the central location of the tree-ring records in northwestern North America analyzed in this study and shown in Figure 1.

Northwest Territories (Beaulieu, 2022), with the weakest cold severity post-1809, had the most (weakly) negative correlation with the PDO and (weakly) positive correlation with the NPI (Figures 5a and 5b). We also observed an association between post-1809 cold severity and the sensitivity of each record to the well-known 1976/1977 regime shift in the PDO/NPI, where tree-ring records with a more extreme cold severity similarly have a stronger response to the regime shift ($r = -0.88$, $p < 0.01$; Figure 5c). In all cases, similar results were obtained when the records were detrended from 1900 to 1990 prior to analysis (Figures S6 and S7 in Supporting Information S1).

At a broader spatial scale, there is also a similarity between the 1810 temperature dipole seen across northern North America (Figure 6a, also shown in Figure 4) and modern teleconnections between surface air temperatures and the

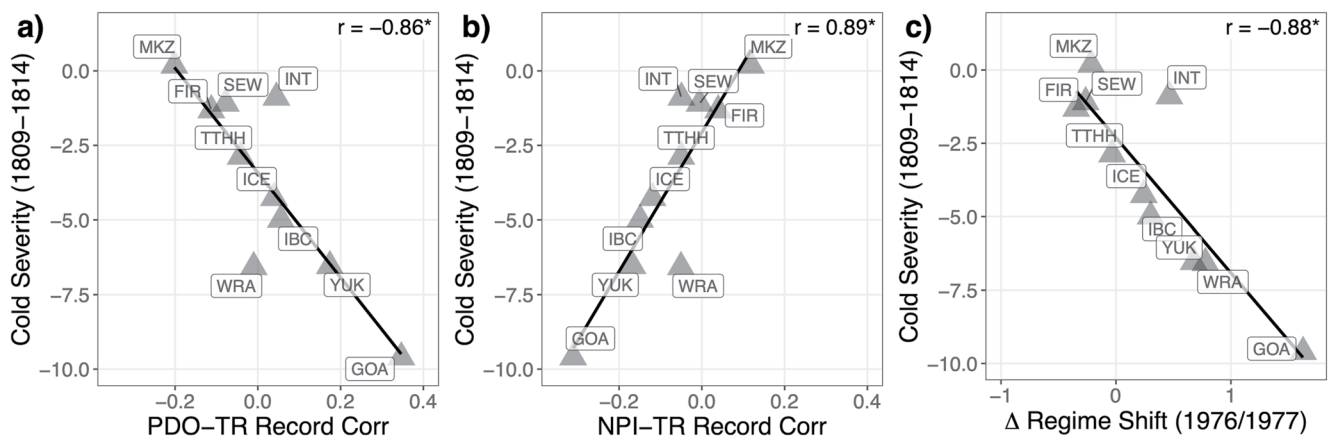

Figure 5. The association between the post-1809 cold severity for each temperature record and sensitivity to Pacific decadal variability during the observational period. The cooling severity for each record was compared against the correlation between each record and the annually averaged Pacific Decadal Oscillation (PDO; a) and the North Pacific Index (NPI; b), as well as the response to the Pacific 1976/1977 regime shift (c). *$p < 0.05$.

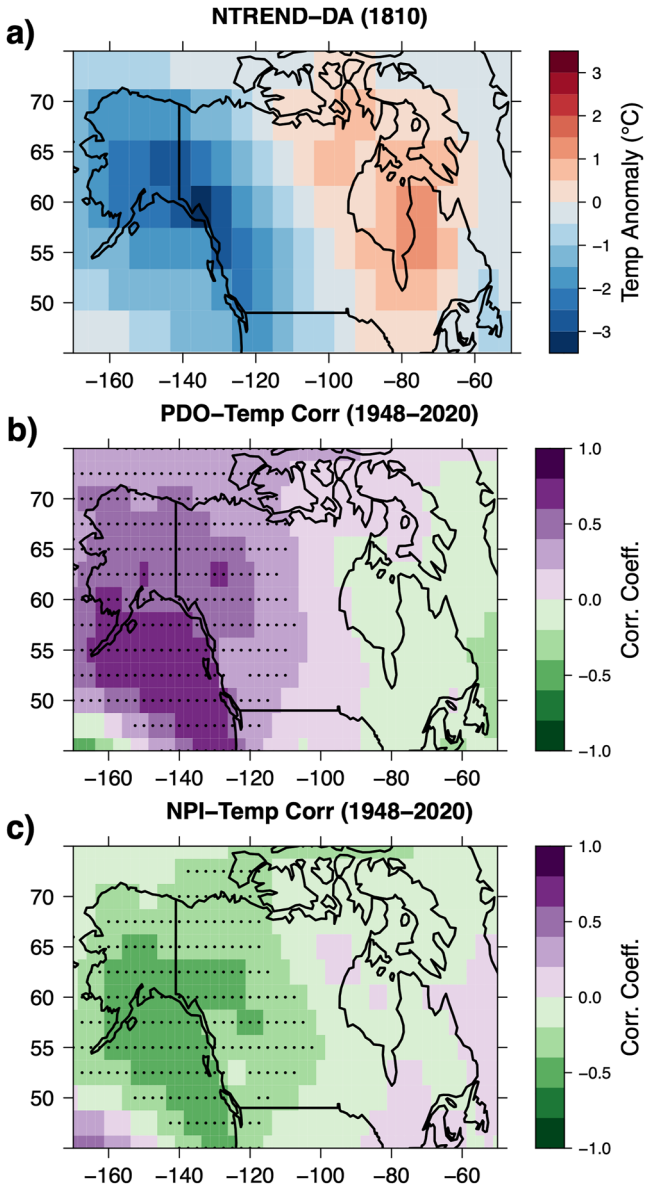

Figure 6. The spatial temperature signature of 1810 across northern North America and spatial correlations between temperatures and measures of Pacific decadal variability. The summer temperature anomalies across northern North America (relative to the 1951–1980 CE mean; King et al., 2021a, 2021b) during the year 1810 are shown in panel (a), and panels (b and c) show correlations between surface air temperature (NCEP/NCAR reanalysis) and the annually averaged PDO and NPI, respectively, from 1948 to 2020. The dots indicate statistical significance at $p < 0.05$.

annually averaged PDO (Figure 6b) and NPI (Figure 6c). There are positive (negative) correlations between the PDO (NPI) and surface air temperatures broadly across the western part of the domain, where cold temperatures were reconstructed for 1810. In the east, where relatively warmer 1810 conditions were reconstructed, there are weak and non-significant negative (positive) correlations with the PDO (NPI). These spatial correlation patterns persisted, though are marginally weaker, after data detrending (Figure S8 in Supporting Information S1). Other climate modes and processes beyond the North Pacific, particularly in the North Atlantic, can have impacts on regional temperatures and circulation patterns across northern North America (e.g., Iles & Hegerl, 2017; McAfee, 2014; Vincent et al., 2015), and could have also contributed to the distinct east-west temperature pattern during that time.

While correlations between the PDO and surface air temperatures during the observational period are strongest in the winter and spring, these relationships can persist well into summer, particularly in southern Alaska and coastal British Columbia (L. E. Fleming & Anchukaitis, 2016; S. W. Fleming & Whitfield, 2010). Similar relationships between cold severity and correlations with the PDO/NPI for averaged cold-season (October - March) and warm-season (April - September) months were observed ($p < 0.01$; Figure S9 in Supporting Information S1). These seasonal relationships were weaker than those using the annually averaged indices, though there was a similarly strong association between warm-season PDO correlations and cold severity ($r = -0.85$, $p < 0.01$, Figure S9b in Supporting Information S1). For NPI, the highest seasonal association was found for the cold season ($r = 0.76$, $p < 0.01$; Figure S9c in Supporting Information S1). We also found that the spatial pattern of correlations between PDO/NPI and surface air temperatures across North America are similar during the cold and warm-season months, though with higher strength and significance during the cold season (Figure S10 in Supporting Information S1). Given the general similarity in seasonal responses, the warm-season temperature reconstructions and records used here are likely still able to reflect aspects of PDO variability.

Taken together, our findings illustrate an association between regional temperature anomalies following the 1809 eruption and the degree of sensitivity to North Pacific decadal variability, at least during the observational period. Assuming the stability of teleconnections (see below), this suggests that a weakened Aleutian low in the North Pacific and related negative PDO-like conditions could have contributed to the spatial pattern of cooling after the eruption, which was most pronounced in the year 1810 (Figures 4 and 6a). The negative phase of the PDO, represented by cool SSTs along the west coast of North America and a weakened Aleutian Low (positive NPI), has been linked to cold temperatures around coastal locations of the North Pacific, particularly coastal Alaska, with a weaker temperature sensitivity in interior locations (S. W. Fleming & Whitfield, 2010).

3.4. Post-1809 Cooling: A Shift to Negative PDO-Like Conditions or Preconditioning From a Background State?

While our results suggest a connection between post-1809 cooling and negative PDO-like conditions, an important question is whether the 1809 volcanic event might have triggered a negative PDO phase, or whether such a climate state already existed and could have contributed to the spatial character of post-volcanic cooling. The association between volcanic forcing and North Pacific decadal variability has been studied in the modeling community, but there is no clear consensus on their relations or lack thereof. Volcanic aerosols from large stratospheric eruptions can impact

climate via shortwave radiative effects (leading to enhanced albedo and surface cooling), stratospheric warming due to increased absorption of longwave radiation, and resulting dynamical responses of atmosphere-ocean processes over decadal or longer time scales (Marshall et al., 2022; Robock, 2000; Zanchettin, 2017). Using an atmosphere-ocean general circulation model, Wang et al. (2012) found that strong volcanic eruptions can induce a negative phase of the PDO via a series of dynamical processes and feedbacks, beginning with an increase in the pole-to-equator temperature gradient in the lower stratosphere. Similarly, a modeling experiment, focusing on the early nineteenth century, found that volcanic forcing induced a negative PDO, and that this response was strengthened when combining both solar and volcanic forcings (Fang et al., 2022). Conversely, modeled PDO did not consistently respond to volcanic forcing in simulations of the last millennium (L. E. Fleming & Anchukaitis, 2016), and simulated north Pacific variability was found to be largely insensitive to natural external forcings (Zanchettin, Rubino, et al., 2013). Regarding the 1809 event specifically, the proxy-model comparison in Timmreck et al. (2021) suggests that the east-west temperature dipole across North America after 1809, also described here, is likely not a result of volcanic forcing, but rather, reflects specific dynamical conditions.

Distinguishing forced versus unforced climate variability, and their relative influence on one another, can also be complicated as, for example, a simulation of oceanic recovery after the eruptions of the late Little Ice Age shows a spatial SST pattern somewhat resembling that of a negative PDO starting 3–7 years after eruptions (Brönnimann et al., 2019). Clarifying the effects of and interactions between large volcanic eruptions and decadal climate variability remains a challenge, in part due to inadequate modeling of internal climate modes (Zanchettin, 2017) and the limitations of existing observations and reconstructions. Background climate conditions are also a critical consideration in assessing regional climate impacts following major volcanic events, as climate responses can depend on, or be amplified by, the initial climate state (e.g., Lehner et al., 2016; Lough & Fritts, 1987; Mackay et al., 2022; Moreno-Chamarro et al., 2015). The phase of prevailing internal modes of variability can have additive effects on the climatic response after major volcanic eruptions and can also influence mechanisms of subsequent atmosphere-ocean processes (Zanchettin et al., 2019; Zanchettin, Bothe, et al., 2013). Relevant to our study, Illing et al. (2018) found that an artificial Pinatubo-like eruption resulted in notable differences in regional climate forecasts depending on the initial climate state, including persistent cooling in the North Pacific basin when the forecast was initialized with a negative phase of the PDO.

It is challenging to ascertain conditions in the North Pacific leading up to and following the 1809 eruption due to the complexity of North Pacific decadal variability and its teleconnections, and disagreements in existing PDO reconstructions prior to the twentieth century (Newman et al., 2016; St. George, 2014; Wise, 2015). While there are indeed some differences in the tree-ring based PDO reconstructions in the early 1800s (Figures S11a–S11f in Supporting Information S1), most (5/6) reconstructions indicate negative PDO-like (cool) conditions in the few years leading up to and following the 1809 eruption. One limitation is that many of the PDO reconstructions include sites from regions analyzed here. However, the Biondi et al. (2001) PDO reconstruction was derived from independent moisture-sensitive tree-ring sites from Southern and Baja California, and suggests negative or neutral PDO-like conditions at the time of the eruption (Figure S11b in Supporting Information S1). A reconstruction of the winter Pacific North American (PNA) pattern based on tree-ring records from western North America shows a positive phase during the early nineteenth century suggesting a deepened Aleutian Low (Trouet & Taylor, 2010) and thus, more positive PDO-like conditions. This result is not consistent with some PDO reconstructions (Figure S11 in Supporting Information S1), and also contrasts with a negative winter PNA pattern in the early nineteenth century identified in an ensemble of coupled climate simulations (Zanchettin et al., 2015). These differences further highlight uncertainties associated with proxy reconstructions and model deficiencies, and the potential role of internal climate variability (Zanchettin et al., 2015).

Nevertheless, several other sources of proxy evidence suggest cold conditions in the northeast Pacific and Gulf of Alaska region around the time of the 1809 eruption. For example, an observed relationship between traumatic resin ducts in tree rings and the NPI/PDO suggests that a particularly weak Aleutian Low (negative PDO) occurred in the early 1800s (Gaglioti et al., 2019). A regime shift detection analysis on the record of traumatic resin ducts suggests that there was a shift from a positive to negative PDO around 1796 that was sustained until 1837 (Gaglioti et al., 2019). The anomalously cold SSTs reported from bivalves in offshore British Columbia from 1809 to 1811 (Edge et al., 2021; Figure 1) is also consistent with a weak Aleutian Low or negative PDO-like conditions along the northeastern Pacific following 1809.

Overall, most of these pieces of paleoclimatic evidence suggest negative PDO-like conditions during and following the 1809 eruption, but in many cases, also indicate negative PDO-like conditions in years leading up to the

1809 eruption. The implication of the latter conclusion is that a state similar to a negative PDO in the North Pacific could have preconditioned or strengthened the spatial cooling response post-eruption (Vargo, 2013), and that the 1809 event might not have directly triggered a shift to a negative PDO. The prolonged volcanic cooling of the North Pacific basin following initial negative PDO conditions described in model experiments (Illing et al., 2018) supports the importance of preconditioning in this region.

3.5. Different Modes of Climate Variability and the 1809 Eruption

Similar to negative PDO-like conditions, a La Niña background state of the equatorial Pacific could have also preconditioned the spatial temperature response in NWNA after 1809. The PDO is partly related to the state of ENSO (Alexander et al., 2002; Newman et al., 2016); often, El Niño (La Niña) conditions are associated with a strengthening (weakening) and southeastward (northwestward) shift of the Aleutian Low (Bjerknes, 1969; Trenberth et al., 1998), and therefore, a positive (negative) phase of the PDO. ENSO teleconnections are similar to those of the PDO in NWNA during the instrumental era (S. W. Fleming & Whitfield, 2010), though the strength of these teleconnections to the North Pacific varies over time (Gershunov & Barnett, 1998), as do interactions between ENSO and other climate systems, which collectively influence spatial climate patterns (D'Arrigo & Wilson, 2006b; Gershunov & Barnett, 1998; Wise, 2015). A Niño3.4 reconstruction (Li et al., 2013a) suggests that La Niña conditions were predominant in the five years leading up the 1809 eruption (Figure S11g in Supporting Information S1), and other reconstructions broadly agree on a cool phase of ENSO at least one year prior to 1809 (e.g., seen in Cook et al., 2018; Dätwyler et al., 2019), also hinting at a potential weakened Aleutian Low as a background state for the 1809 eruption. Coral SST reconstructions disagree on the state of the eastern tropical Pacific, but do show consistent cooling in the early 1800s in the tropical western Pacific and Indian Oceans coinciding with the 1809 unidentified eruption and Tambora (Tierney et al., 2015). Instrumental marine air temperatures in the tropics also suggest cooling in both 1809 and the "year without a summer," 1816 (Chenoweth, 2001). However, in contrast to the 1809 eruption, the mild temperatures across NWNA in 1816 could have been linked with warmer El Niño conditions in the equatorial Pacific following Tambora (Figure S11g in Supporting Information S1), as suggested by some studies (D'Arrigo et al., 2009; Dätwyler et al., 2019; Li et al., 2013a; Wilson et al., 2006); El Niño conditions during that time are also consistent with inferences based on drought reconstructions from Asia and the Americas (Anchukaitis et al., 2010; E. R. Cook, Anchukaitis, et al., 2010a; E. R. Cook, Seager, et al., 2010; Wegmann et al., 2014) although coral SST reconstructions in the eastern tropical Pacific once again are uncertain (Tierney et al., 2015).

In addition to direct reconstructions of climate modes, spatial hydroclimate patterns from 1809 to 1810 based on three gridded drought reconstructions (NADA, OWDA, and MADA; E. R. Cook, Anchukaitis, et al., 2010a, 2010b; E. R. Cook, Seager, et al., 2010; E. R. Cook, Seager, Heim, et al., 2015; E. R. Cook, Seager, Kushnir, et al., 2015) provide further support for a cold Pacific (negative ENSO, negative PDO), as well as a negative phase of the North Atlantic Oscillation (NAO) associated with the eruption (Figure S12 in Supporting Information S1). The anomalous wet conditions in NWNA and in tropical Asia in 1809 and 1810 are typically associated with cold phases of ENSO and/or the PDO (Baek et al., 2017; Coats et al., 2016; E. R. Cook, Anchukaitis, et al., 2010a; McCabe et al., 2004). In Europe, the Mediterranean, and North Africa, the spatial drought pattern in summer PDSI in the OWDA (E. R. Cook, Seager, Heim, et al., 2015; E. R. Cook, Seager, Kushnir, et al., 2015) is consistent with a negative phase of the NAO and the East Atlantic Pattern, colder Atlantic SSTs, and upper level westerly winds displaced toward the south (Anchukaitis et al., 2019; Rao et al., 2017). This could have had impacts on regional climate anomalies in eastern North America, in particular, and should be explored. The post-1809 hydroclimatic signatures apparent in the gridded drought reconstructions provide additional support for the dynamics potentially driving the spatial pattern of temperature anomalies identified in NWNA, and further analysis could be beneficial for assessing the post-1809 climate patterns in other regions in detail.

4. Conclusions

Our network analysis of NWNA tree-ring temperature reconstructions shows that the Gulf of Alaska, the southern Yukon, and sites broadly proximal to the northeastern Pacific Ocean experienced extreme cold following the unidentified 1809 eruption, particularly in the year 1810. The severity of cold conditions diminishes away from this region and temperatures were relatively mild along the northernmost portion of the NWNA tree-ring network and the eastern half of North America. We find that the post-1809 spatial temperature patterns resemble

modern-day teleconnections associated with a negative PDO and a weakened Aleutian Low, suggesting that North Pacific dynamics influenced the spatial pattern of the post-volcanic climate response. It is not entirely certain, however, whether a large volcanic eruption in 1809 could have forced a transition to negative PDO-like conditions or whether a pre-existing negative PDO could have modified the direct radiative impacts. However, many paleoclimate data sets do indicate colder conditions in the Northeast Pacific preceded the 1809 eruption and these background conditions may have strengthened or augmented the spatial cooling pattern (e.g., Vargo, 2013). Constraining the timing and locations of the unidentified 1809 eruption(s), the structure of the atmospheric forcing (Timmreck et al., 2021), and regional climate dynamics and historical impacts in NWNA during the early nineteenth century, will be essential for understanding the mechanisms behind extreme cold conditions in NWNA during the late Little Ice Age, and implications of volcanism on regional climate variability.

Conflict of Interest

The authors declare no conflicts of interest relevant to this study.

Data Availability Statement

A network of ten tree-ring data sets were used in this study and are described in Table 1. The data sets are available as follows: Interior British Columbia (IBC; Wilson et al., 2014; Wilson, Rao, et al., 2016), Icefields (ICE; Luckman & Wilson, 2005a, 2005b), Gulf of Alaska (GOA; Wilson et al., 2017, 2023), Southern Yukon (YUK; Wilson et al., 2019a, 2019b), Wrangell Mountains (WRA; Davi et al., 2003a, 2003b), Twisted Tree-Heartrot Hill (TTHH; D'Arrigo & Jacoby, 1999, 2023), Seward Peninsula (SEW; D'Arrigo et al., 2004, 2023), Interior Alaska (INT; Jacoby et al., 1999, 2023), Mackenzie Delta (MKZ; Beaulieu, 2022, 2023), and Firth River (FIR; Anchukaitis et al., 2013a, 2013b). Figures and maps were created with the R Project for Statistical Computing software (version 4.1.0; R Core Team, 2021) and spatial correlations with the NCEP/NCAR reanalysis data were computed with the Physical Science Laboratory's Climate Plotting and Analysis Tool (https://psl.noaa.gov/data/correlation/). Regarding PDO/NPI indices, we used the Mantua PDO index provided by the Joint Institute for the Study of the Atmosphere and Ocean (Mantua, 2018) and the Trenberth and Hurrell North Pacific Index from the National Center of Atmospheric Research (NCAR, 2022; Trenberth & Hurrell, 1994). The NTREND summer temperature field reconstruction (Anchukaitis et al., 2017; Wilson, Anchukaitis, et al., 2016b) and the NTEND-DA (King et al., 2021a, 2021b) were also analyzed here. PDO/Nino3.4 index reconstructions include: D'Arrigo et al. (2001, 2002), Biondi et al. (1998, 2001), MacDonald and Case (2005a, 2005b), D'Arrigo and Wilson (2006a, 2006b), Evans et al. (2001, 2003), and Li et al. (2013a, 2013b). The drought atlases analyzed in this study include: the Old World Drought Atlas (E. R. Cook, 2015; E. R. Cook, Seager, Kushnir, et al., 2015); North America Drought Atlas (Living Blended Drought Atlas—E. R. Cook, Seager, et al., 2010; E. R. Cook, Seager, Heim, et al., 2015); and the Monsoon Asia Drought Atlas (E. R. Cook, Anchukaitis, et al., 2010a, 2010b).

Acknowledgments
We would like to thank members of the Lamont-Doherty Earth Observatory Tree-ring Lab for valuable discussions and feedback on this research. This research was funded by the National Science Foundation (NSF) Arctic Social Science (Grants 2112463 and 2112314). KJA was supported by NSF AGS-1501834 and AGS-2102993. RD, KA, LAH, and BVG were supported by NSF OPP #2124885. GW and BVG were supported by NSF P2C2 #2002561. TJP was supported by NSERC Discovery Grant RGPIN-2016-06730. RW was supported by NERC project #NE/S000887/1. MPR was supported by NOAA Climate and Global Change Postdoctoral Fellowship Program, UCAR-CPAESS award #NA18NWS4620043B and EU2020 Marie Skłodowska-Curie Grant 101031748.

References

Adamson, G. C. D. (2015). Private diaries as information sources in climate research. *WIREs Climate Change*, *6*(6), 599–611. https://doi.org/10.1002/wcc.365

Alexander, M. A., Bladé, I., Newman, M., Lanzante, J. R., Lau, N.-C., & Scott, J. D. (2002). The atmospheric bridge: The influence of ENSO teleconnections on air–sea interaction over the global oceans. *Journal of Climate*, *15*(16), 2205–2231. https://doi.org/10.1175/1520-0442(2002)015<2205:TABTIO>2.0.CO;2

Anchukaitis, K. J., Breitenmoser, P., Briffa, K. R., Buchwal, A., Büntgen, U., Cook, E. R., et al. (2012). Tree rings and volcanic cooling. *Nature Geoscience*, *5*(12), 836–837. https://doi.org/10.1038/ngeo1645

Anchukaitis, K. J., Buckley, B. M., Cook, E. R., Cook, B. I., D'Arrigo, R. D., & Ammann, C. M. (2010). Influence of volcanic eruptions on the climate of the Asian monsoon region. *Geophysical Research Letters*, *37*(22), L22703. https://doi.org/10.1029/2010GL044843

Anchukaitis, K. J., Cook, E. R., Cook, B. I., Pearl, J., D'Arrigo, R., & Wilson, R. (2019). Coupled modes of North Atlantic Ocean-atmosphere variability and the onset of the Little Ice Age. *Geophysical Research Letters*, *46*(21), 12417–12426. https://doi.org/10.1029/2019GL084350

Anchukaitis, K. J., D'Arrigo, R. D., Andreu-Hayles, L., Frank, D., Verstege, A., Curtis, A., et al. (2013a). NOAA/WDS paleoclimatology - Firth River Alaska 930 year maximum latewood density temperature reconstruction [Dataset]. NOAA National Centers for Environmental Information. https://doi.org/10.25921/skjn-w996

Anchukaitis, K. J., D'Arrigo, R. D., Andreu-Hayles, L., Frank, D., Verstege, A., Curtis, A., et al. (2013b). Tree-ring-reconstructed summer temperatures from northwestern North America during the last nine centuries. *Journal of Climate*, *26*(10), 3001–3012. https://doi.org/10.1175/JCLI-D-11-00139.1

Anchukaitis, K. J., & Smerdon, J. E. (2022). Progress and uncertainties in global and hemispheric temperature reconstructions of the Common Era. *Quaternary Science Reviews*, *286*, 107537. https://doi.org/10.1016/j.quascirev.2022.107537

Anchukaitis, K. J., Wilson, R., Briffa, K. R., Büntgen, U., Cook, E. R., D'Arrigo, R., et al. (2017). Last millennium Northern Hemisphere summer temperatures from tree rings: Part II, spatially resolved reconstructions. *Quaternary Science Reviews*, *163*, 1–22. https://doi.org/10.1016/j.quascirev.2017.02.020

Anderson, P., & Piatt, J. (1999). Community reorganization in the Gulf of Alaska following ocean climate regime shift. *Marine Ecology Progress Series*, *189*, 117–123. https://doi.org/10.3354/meps189117

Appleton, S. N., & St. George, S. (2018). High-elevation mountain hemlock growth as a surrogate for cool-season precipitation in Crater Lake National Park, USA. *Dendrochronologia*, *52*, 20–28. https://doi.org/10.1016/j.dendro.2018.09.003

Baek, S. H., Smerdon, J. E., Coats, S., Williams, A. P., Cook, B. I., Cook, E. R., & Seager, R. (2017). Precipitation, temperature, and teleconnection signals across the combined North American, monsoon Asia, and old world drought atlases. *Journal of Climate*, *30*(18), 7141–7155. https://doi.org/10.1175/JCLI-D-16-0766.1

Beaulieu, S. (2022). *Summer climate reconstruction using tree-ring blue intensity in the Mackenzie Delta, Northwest Territories* (MSc Thesis). University of Toronto. Retrieved from https://hdl.handle.net/1807/124897

Beaulieu, S. (2023). Summer climate reconstruction using tree-ring blue intensity in the Mackenzie Delta, Northwest Territories [Dataset]. Borealis. https://doi.org/10.5683/SP3/05DYXB

Biondi, F., Gershunov, A., & Cayan, D. R. (1998). NOAA/WDS Paleoclimatology - Biondi et al. 2001 Pacific Decadal Oscillation Reconstruction [Dataset]. NOAA National Centers for Environmental Information. https://doi.org/10.25921/jeq5-bx19

Biondi, F., Gershunov, A., & Cayan, D. R. (2001). North Pacific decadal climate variability since 1661. *Journal of Climate*, *14*(1), 5–10. https://doi.org/10.1175/1520-0442(2001)014<0005:NPDCVS>2.0.CO;2

Bjerknes, J. (1969). Atmospheric teleconnections from the equatorial Pacific. *Monthly Weather Review*, *97*(3), 163–172. https://doi.org/10.1175/1520-0493(1969)097<0163:ATFTEP>2.3.CO;2

Blong, R. J. (1982). *The time of darkness: Local legends and volcanic reality in Papua New Guinea*. Australian National University Press.

Briffa, K. R., Jones, P. D., & Schweingruber, F. H. (1992). Tree-ring density reconstructions of summer temperature patterns across western North America since 1600. *Journal of Climate*, *5*(7), 735–754. https://doi.org/10.1175/1520-0442(1992)005<0735:trdros>2.0.co;2

Briffa, K. R., Jones, P. D., & Schweingruber, F. H. (1994). Summer temperatures across northern North America: Regional reconstructions from 1760 using tree-ring densities. *Journal of Geophysical Research*, *99*(D12), 25835. https://doi.org/10.1029/94JD02007

Brönnimann, S., Franke, J., Nussbaumer, S. U., Zumbühl, H. J., Steiner, D., Trachsel, M., et al. (2019). Last phase of the Little Ice Age forced by volcanic eruptions. *Nature Geoscience*, *12*(8), 650–656. https://doi.org/10.1038/s41561-019-0402-y

Brönnimann, S., & Krämer, D. (2016). *Tambora and the "Year Without a Summer" of 1816. A perspective on earth and human systems science* (Vol. 90). Geographica Bernensia.

Büntgen, U., Allen, K., Anchukaitis, K. J., Arseneault, D., Boucher, É., Bräuning, A., et al. (2021). The influence of decision-making in tree ring-based climate reconstructions. *Nature Communications*, *12*(1), 3411. https://doi.org/10.1038/s41467-021-23627-6

Chenoweth, M. (2001). Two major volcanic cooling episodes derived from global marine air temperature, AD 1807–1827. *Geophysical Research Letters*, *28*(15), 2963–2966. https://doi.org/10.1029/2000GL012648

Coats, S., Smerdon, J. E., Cook, B. I., Seager, R., Cook, E. R., & Anchukaitis, K. J. (2016). Internal ocean-atmosphere variability drives megadroughts in Western North America. *Geophysical Research Letters*, *43*(18), 9886–9894. https://doi.org/10.1002/2016GL070105

Cole-Dai, J., Ferris, D., Lanciki, A., Savarino, J., Baroni, M., & Thiemens, M. H. (2009). Cold decade (AD 1810–1819) caused by Tambora (1815) and another (1809) stratospheric volcanic eruption. *Geophysical Research Letters*, *36*(22), L22703. https://doi.org/10.1029/2009GL040882

Cook, B. I., Williams, A. P., Smerdon, J. E., Palmer, J. G., Cook, E. R., Stahle, D. W., & Coats, S. (2018). Cold tropical Pacific sea surface temperatures during the late sixteenth-century North American megadrought. *Journal of Geophysical Research: Atmospheres*, *123*(20), 11307–11320. https://doi.org/10.1029/2018JD029323

Cook, E. R. (2015). NOAA/WDS paleoclimatology - Old world drought atlas [Dataset]. NOAA National Centers for Environmental Information. https://doi.org/10.25921/rjm6-mq74

Cook, E. R., Anchukaitis, K. J., Buckley, B. M., D'Arrigo, R. D., Jacoby, G. C., & Wright, W. E. (2010a). Asian Monsoon failure and megadrought during the last millennium. *Science*, *328*(5977), 486–489. https://doi.org/10.1126/science.1185188

Cook, E. R., Anchukaitis, K. J., Buckley, B. M., D'Arrigo, R. D., Jacoby, G. C., & Wright, W. E. (2010b). NOAA/WDS Paleoclimatology - Monsoon Asia Drought Atlas (MADA) [Dataset]. NOAA National Centers for Environmental Information. https://doi.org/10.25921/b8gk-7h90

Cook, E. R., & Krusic, P. J. (2020). RCSsigfree (version 49v1).

Cook, E. R., Seager, R., Heim, R. R., Vose, R. S., Herweijer, C., & Woodhouse, C. (2010). Megadroughts in North America: Placing IPCC projections of hydroclimatic change in a long-term palaeoclimate context. *Journal of Quaternary Science*, *25*(1), 48–61. https://doi.org/10.1002/jqs.1303

Cook, E. R., Seager, R., Heim, R. R., Vose, R. S., Herweijer, C., & Woodhouse, C. (2015). NOAA/WDS Paleoclimatology - The "Living Blended Drought Atlas (LBDA)" North American drought reconstruction for the last 2000 years [Dataset]. NOAA National Centers for Environmental Information. Retrieved from https://www.ncei.noaa.gov/access/paleo-search/study/19119

Cook, E. R., Seager, R., Kushnir, Y., Briffa, K. R., Büntgen, U., Frank, D., et al. (2015). Old World megadroughts and pluvials during the Common Era. *Science Advances*, *1*(10), e1500561. https://doi.org/10.1126/sciadv.1500561

Crowley, T. J., Obrochta, S. P., & Liu, J. (2014). Recent global temperature "plateau" in the context of a new proxy reconstruction. *Earth's Future*, *2*(5), 281–294. https://doi.org/10.1002/2013EF000216

Cruikshank, J. (2001). Glaciers and climate change: Perspectives from oral tradition. *Arctic*, *54*(4), 377–393. https://doi.org/10.14430/arctic795

Cruikshank, J. (2007). *Do glaciers listen?: Local knowledge, colonial encounters, and social imagination*. University of British Columbia Press.

Dai, J., Mosley-Thompson, E., & Thompson, L. G. (1991). Ice core evidence for an explosive tropical volcanic eruption 6 years preceding Tambora. *Journal of Geophysical Research*, *96*(D9), 17361–17366. https://doi.org/10.1029/91jd01634

D'Arrigo, R., & Jacoby, G. (1999). Northern North American tree-ring evidence for regional temperature changes after major volcanic events. *Climatic Change*, *41*(1), 1–15. https://doi.org/10.1023/A:1005370210796

D'Arrigo, R., & Jacoby, G. (2023). NOAA/WDS Paleoclimatology - D'Arrigo - Twisted Tree Heartrot Hill Update - PCGL - ITRDB CAN680 [Dataset]. NOAA National Centers for Environmental Information. https://www.ncei.noaa.gov/access/paleo-search/study/37665

D'Arrigo, R., Klinger, P., Newfield, T., Rydval, M., & Wilson, R. (2020). Complexity in crisis: The volcanic cold pulse of the 1690s and the consequences of Scotland's failure to cope. *Journal of Volcanology and Geothermal Research*, *389*, 106746. https://doi.org/10.1016/j.jvolgeores.2019.106746

D'Arrigo, R., Mashig, E., Frank, D., Jacoby, G., & Wilson, R. (2004). Reconstructed warm season temperatures for Nome, Seward Peninsula, Alaska. *Geophysical Research Letters*, *31*(9), L09202. https://doi.org/10.1029/2004GL019756

D'Arrigo, R., Mashig, E., Frank, D., Jacoby, G., & Wilson, R. (2023). NOAA/WDS Paleoclimatology - Reconstructed warm season temperatures for Nome, Seward Peninsula, Alaska from 1389–2001 CE [Dataset]. NOAA National Centers for Environmental Information. https://www.ncei.noaa.gov/access/paleo-search/study/37668

D'Arrigo, R., Villalba, R., & Wiles, G. (2001). Tree-ring estimates of Pacific decadal climate variability. *Climate Dynamics*, *18*(3), 219–224. https://doi.org/10.1007/s003820100177

D'Arrigo, R., Villalba, R., & Wiles, G. (2002). NOAA/WDS Paleoclimatology - D'Arrigo et al. 2001 Pacific Decadal Oscillation Reconstruction [Dataset]. NOAA National Centers for Environmental Information. https://doi.org/10.25921/g4tx-3d90

D'Arrigo, R., & Wilson, R. (2006a). NOAA/WDS Paleoclimatology - D'Arrigo and Wilson 2006 Spring Pacific Decadal Oscillation Index Reconstruction [Dataset]. NOAA National Centers for Environmental Information. https://doi.org/10.25921/47sr-rb68

D'Arrigo, R., & Wilson, R. (2006b). On the Asian expression of the PDO. *International Journal of Climatology*, *26*(12), 1607–1617. https://doi.org/10.1002/joc.1326

D'Arrigo, R., Wilson, R., & Anchukaitis, K. J. (2013). Volcanic cooling signal in tree ring temperature records for the past millennium: Volcanism and tree ring records. *Journal of Geophysical Research: Atmospheres*, *118*(16), 9000–9010. https://doi.org/10.1002/jgrd.50692

D'Arrigo, R., Wilson, R., Palmer, J., Krusic, P., Curtis, A., Sakulich, J., et al. (2006). The reconstructed Indonesian warm pool sea surface temperatures from tree rings and corals: Linkages to Asian monsoon drought and El Niño-Southern Oscillation. *Paleoceanography*, *21*(3), PA3005. https://doi.org/10.1029/2005PA001256

D'Arrigo, R., Wilson, R., & Tudhope, A. (2009). The impact of volcanic forcing on tropical temperatures during the past four centuries. *Nature Geoscience*, *2*(1), 51–56. https://doi.org/10.1038/ngeo393

Dätwyler, C., Abram, N. J., Grosjean, M., Wahl, E. R., & Neukom, R. (2019). El Niño–Southern Oscillation variability, teleconnection changes and responses to large volcanic eruptions since AD 1000. *International Journal of Climatology*, *39*(5), 2711–2724. https://doi.org/10.1002/joc.5983

Davi, N., Jacoby, G. C., & Wiles, G. (2003a). Boreal temperature variability inferred from maximum latewood density and tree-ring width data, Wrangell Mountain region, Alaska. *Quaternary Research*. https://doi.org/10.1016/S0033-5894(03)00115-7

Davi, N., Jacoby, G. C., & Wiles, G. (2003b). NOAA/WDS Paleoclimatology - Davi et al. 2003 Wrangell Mountains Warm Season Temperature Reconstruction [Dataset]. NOAA National Centers for Environmental Information. https://doi.org/10.25921/dgdn-r219

Degroot, D., Anchukaitis, K., Bauch, M., Burnham, J., Carnegy, F., Cui, J., et al. (2021). Towards a rigorous understanding of societal responses to climate change. *Nature*, *591*(7851), 539–550. https://doi.org/10.1038/s41586-021-03190-2

Di Cosmo, N., Hessl, A., Leland, C., Byambasuren, O., Tian, H., Nachin, B., et al. (2018). Environmental stress and steppe nomads: Rethinking the history of the Uyghur Empire (744–840) with paleoclimate data. *Journal of Interdisciplinary History*, *48*(4), 439–463. https://doi.org/10.1162/jinh_a_01194

Dracup, J. A., Lee, K. S., & Paulson, E. G. (1980). On the definition of droughts. *Water Resources Research*, *16*(2), 297–302. https://doi.org/10.1029/WR016i002p00297

Ebbesmeyer, C. C., Cayan, D. R., McLain, D. R., Nichols, F. H., Peterson, D. H., & Redmond, K. T. (1991). 1976 step in the Pacific climate: Forty environmental changes between 1968–1975 and 1977–1984. In *Proceedings of the 7th Annual Pacific Climate Workshop* (pp. 115–126). California Dept of Water Research.

Edge, D. C., Reynolds, D. J., Wanamaker, A. D., Griffin, D., Bureau, D., Outridge, C., et al. (2021). A multicentennial proxy record of Northeast Pacific sea surface temperatures from the annual growth increments of *Panopea generosa*. *Paleoceanography and Paleoclimatology*, *36*(9), e2021PA004291. https://doi.org/10.1029/2021PA004291

Edwards, J., Anchukaitis, K. J., Zambri, B., Andreu-Hayles, L., Oelkers, R., D'Arrigo, R., & von Arx, G. (2021). Intra-annual climate anomalies in northwestern North America following the 1783–1784 CE Laki eruption. *Journal of Geophysical Research: Atmospheres*, *126*(3), e2020JD033544. https://doi.org/10.1029/2020JD033544

Esper, J., Schneider, L., Smerdon, J. E., Schöne, B. R., & Büntgen, U. (2015). Signals and memory in tree-ring width and density data. *Dendrochronologia*, *35*, 62–70. https://doi.org/10.1016/j.dendro.2015.07.001

Evans, M. N., Cane, M. A., & Kaplan, A. (2003). NOAA/WDS Paleoclimatology - Evans et al. 2002 Proxy-Based Pacific SST Reconstructions [Dataset]. NOAA National Centers for Environmental Information. https://doi.org/10.25921/hah6-ys18

Evans, M. N., Cane, M. A., Schrag, D. P., Kaplan, A., Linsley, B. K., Villalba, R., & Wellington, G. M. (2001). Support for tropically-driven Pacific decadal variability based on paleoproxy evidence. *Geophysical Research Letters*, *28*(19), 3689–3692. https://doi.org/10.1029/2001GL013223

Fang, S.-W., Timmreck, C., Jungclaus, J., Krüger, K., & Schmidt, H. (2022). On the additivity of climate responses to the volcanic and solar forcing in the early 19th century (preprint), *Dynamics of the Earth system: Interactions*. https://doi.org/10.5194/egusphere-2022-638

Fleming, L. E., & Anchukaitis, K. J. (2016). North Pacific decadal variability in the CMIP5 last millennium simulations. *Climate Dynamics*, *47*(12), 3783–3801. https://doi.org/10.1007/s00382-016-3041-7

Fleming, S. W., & Whitfield, P. H. (2010). Spatiotemporal mapping of ENSO and PDO surface meteorological signals in British Columbia, Yukon, and southeast Alaska. *Atmosphere-Ocean*, *48*(2), 122–131. https://doi.org/10.3137/AO1107.2010

Forbes, V., Ledger, P. M., Cretu, D., & Elias, S. (2020). A sub-centennial, Little Ice Age climate reconstruction using beetle subfossil data from Nunalleq, southwestern Alaska. *Quaternary International*, *549*, 118–129. https://doi.org/10.1016/j.quaint.2019.07.011

Fuentes, M., Salo, R., Björklund, J., Seftigen, K., Zhang, P., Gunnarson, B., et al. (2018). A 970-year-long summer temperature reconstruction from Rogen, west-central Sweden, based on blue intensity from tree rings. *The Holocene*, *28*(2), 254–266. https://doi.org/10.1177/0959683617721322

Gaglioti, B. V., Mann, D. H., Williams, A. P., Wiles, G. C., Stoffel, M., Oelkers, R., et al. (2019). Traumatic resin ducts in Alaska mountain hemlock trees provide a new proxy for winter storminess. *Journal of Geophysical Research: Biogeosciences*, *124*(7), 1923–1938. https://doi.org/10.1029/2018JG004849

Gedalof, Z., & Smith, D. J. (2001). Interdecadal climate variability and regime-scale shifts in Pacific North America. *Geophysical Research Letters*, *28*(8), 1515–1518. https://doi.org/10.1029/2000GL011779

Gershunov, A., & Barnett, T. P. (1998). Interdecadal modulation of ENSO teleconnections. *Bulletin of the American Meteorological Society*, *79*(12), 12–2725. https://doi.org/10.1175/1520-0477(1998)079<2715:imoet>2.0.co;2

Grove, J. M. (1988). *1988: The Little Ice Age*. Methuen.

Guevara-Murua, A., Williams, C. A., Hendy, E. J., Rust, A. C., & Cashman, K. V. (2014). Observations of a stratospheric aerosol *veil* from a tropical volcanic eruption in December 1808: Is this the *unknown* ~1809 eruption? *Climate of the Past*, *10*(5), 1707–1722. https://doi.org/10.5194/cp-10-1707-2014

Guillet, S., Corona, C., Stoffel, M., Khodri, M., Lavigne, F., Ortega, P., et al. (2017). Climate response to the Samalas volcanic eruption in 1257 revealed by proxy records. *Nature Geoscience*, *10*(2), 123–128. https://doi.org/10.1038/ngeo2875

Harington, C. R. (1992). Year without a summer. World climate in 1816.

Harris, I., Osborn, T. J., Jones, P., & Lister, D. (2020). Version 4 of the CRU TS monthly high-resolution gridded multivariate climate dataset. *Scientific Data*, *7*(1), 109. https://doi.org/10.1038/s41597-020-0453-3

Heeter, K. J., Harley, G. L., Maxwell, J. T., Wilson, R. J., Abatzoglou, J. T., Rayback, S. A., et al. (2021). Summer temperature variability since 1730 CE across the low-to-mid latitudes of western North America from a tree ring blue intensity network. *Quaternary Science Reviews*, *267*, 107064. https://doi.org/10.1016/j.quascirev.2021.107064

Iles, C., & Hegerl, G. (2017). Role of the North Atlantic Oscillation in decadal temperature trends. *Environmental Research Letters*, *12*(11), 114010. https://doi.org/10.1088/1748-9326/aa9152

Illing, S., Kadow, C., Pohlmann, H., & Timmreck, C. (2018). Assessing the impact of a future volcanic eruption on decadal predictions. *Earth System Dynamics*, *9*(2), 701–715. https://doi.org/10.5194/esd-9-701-2018

Jacoby, G. C., Workman, K. W., & D'Arrigo, R. D. (1999). Laki eruption of 1783, tree rings, and disaster for northwest Alaska Inuit. *Quaternary Science Reviews*, *18*(12), 1365–1371. https://doi.org/10.1016/S0277-3791(98)00112-7

Jacoby, G. C., & Cook, E. R. (1981). Past temperature variations inferred from a 400-year tree-ring chronology from Yukon Territory, Canada. *Arctic and Alpine Research*, *13*(4), 409. https://doi.org/10.2307/1551051

Jacoby, G. C., Workman, K. W., & D'Arrigo, R. D. (2023). NOAA/WDS Paleoclimatology - warm-season temperature reconstruction for Northern Alaska from 1680–1990 CE [Dataset]. NOAA National Centers for Environmental Information. Retrieved from https://www.ncei.noaa.gov/access/paleo-search/study/37667

King, J. M., Anchukaitis, K. J., Tierney, J. E., Hakim, G. J., Emile-Geay, J., Zhu, F., & Wilson, R. (2021a). A data assimilation approach to last millennium temperature field reconstruction using a limited high-sensitivity proxy network. *Journal of Climate*, *34*(17), 7091–7111. https://doi.org/10.1175/JCLI-D-20-0661.1

King, J. M., Anchukaitis, K. J., Tierney, J. E., Hakim, G. J., Emile-Geay, J., Zhu, F., & Wilson, R. (2021b). NOAA/WDS Paleoclimatology - Northern Hemisphere 1262 year NTREND assimilation surface temperature reconstructions [Dataset]. NOAA National Centers for Environmental Information. https://doi.org/10.25921/vey7-kx38

Krech, S. (1978a). Disease, starvation, and Northern Athapaskan social organization. *American Ethnologist*, *5*(4), 710–732. https://doi.org/10.1525/ae.1978.5.4.02a00050

Krech, S. (1978b). On the aboriginal population of the Kutchin. *Arctic Anthropology*, 89–104.

Lehner, F., Schurer, A. P., Hegerl, G. C., Deser, C., & Frölicher, T. L. (2016). The importance of ENSO phase during volcanic eruptions for detection and attribution. *Geophysical Research Letters*, *43*(6), 2851–2858. https://doi.org/10.1002/2016GL067935

Li, J., Xie, S.-P., Cook, E. R., Morales, M. S., Christie, D. A., Johnson, N. C., et al. (2013a). El Niño modulations over the past seven centuries. *Nature Climate Change*, *3*(9), 822–826. https://doi.org/10.1038/nclimate1936

Li, J., Xie, S.-P., Cook, E. R., Morales, M. S., Christie, D. A., Johnson, N. C., et al. (2013b). NOAA/WDS Paleoclimatology - 700 Year El Niño/Southern Oscillation (ENSO) Niño3.4 index reconstruction [Dataset]. NOAA National Centers for Environmental Information. https://doi.org/10.25921/jfqm-9178

Liang, E., Liu, X., Yuan, Y., Qin, N., Fang, X., Huang, L., et al. (2006). The 1920s drought recorded by tree rings and historical documents in the semi-arid and arid areas of Northern China. *Climatic Change*, *79*(3–4), 403–432. https://doi.org/10.1007/s10584-006-9082-x

Lough, J. M., & Fritts, H. C. (1987). An assessment of the possible effects of volcanic eruptions on North American climate using tree-ring data, 1602 to 1900 AD. *Climatic Change*, *10*(3), 219–239. https://doi.org/10.1007/BF00143903

Lücke, L. J., Hegerl, G. C., Schurer, A. P., & Wilson, R. (2019). Effects of memory biases on variability of temperature reconstructions. *Journal of Climate*, *32*(24), 8713–8731. https://doi.org/10.1175/JCLI-D-19-0184.1

Luckman, B. H., & Wilson, R. J. S. (2005a). NOAA/WDS Paleoclimatology - Luckman and Wilson 2005 Canadian Rockies Summer Temperature Reconstruction [Dataset]. NOAA National Centers for Environmental Information. https://doi.org/10.25921/w7rj-z103

Luckman, B. H., & Wilson, R. J. S. (2005b). Summer temperatures in the Canadian Rockies during the last millennium: A revised record. *Climate Dynamics*, *24*(2–3), 131–144. https://doi.org/10.1007/s00382-004-0511-0

MacDonald, G. M., & Case, R. (2005a). NOAA/WDS Paleoclimatology - MacDonald and case 2005 Pacific Decadal Oscillation Reconstruction for the Past Millennium [Dataset]. NOAA National Centers for Environmental Information. https://doi.org/10.25921/7eks-pq18

MacDonald, G. M., & Case, R. (2005b). Variations in the Pacific Decadal Oscillation over the past millennium. *Geophysical Research Letters*, *32*(8), L08703. https://doi.org/10.1029/2005GL022478

Mackay, H., Plunkett, G., Jensen, B. J. L., Aubry, T. J., Corona, C., Kim, W. M., et al. (2022). The 852/3 CE Mount Churchill eruption: Examining the potential climatic and societal impacts and the timing of the medieval climate anomaly in the North Atlantic region. *Climate of the Past*, *18*(6), 1475–1508. https://doi.org/10.5194/cp-18-1475-2022

Mantua, N. J. (2018). PDO index [Dataset]. Joint Institute for the Study of the Atmosphere and Ocean. Retrieved from http://research.jisao.washington.edu/pdo/PDO.latest.txt

Mantua, N. J., Hare, S. R., Zhang, Y., Wallace, J. M., & Francis, R. C. (1997). A Pacific Interdecadal Climate Oscillation with impacts on Salmon production. *Bulletin of the American Meteorological Society*, *78*(6), 1069–1080. https://doi.org/10.1175/1520-0477(1997)078<1069:apicow>2.0.co;2

Marshall, L. R., Maters, E. C., Schmidt, A., Timmreck, C., Robock, A., & Toohey, M. (2022). Volcanic effects on climate: Recent advances and future avenues. *Bulletin of Volcanology*, *84*(5), 54. https://doi.org/10.1007/s00445-022-01559-3

McAfee, S. A. (2014). Consistency and the lack Thereof in Pacific decadal oscillation impacts on North American winter climate. *Journal of Climate*, *27*(19), 7410–7431. https://doi.org/10.1175/JCLI-D-14-00143.1

McCabe, G. J., Palecki, M. A., & Betancourt, J. L. (2004). Pacific and Atlantic Ocean influences on multidecadal drought frequency in the United States. *Proceedings of the National Academy of Sciences*, *101*(12), 4136–4141. https://doi.org/10.1073/pnas.0306738101

Melvin, T. M., & Briffa, K. R. (2008). A "signal-free" approach to dendroclimatic standardisation. *Dendrochronologia*, *26*(2), 71–86. https://doi.org/10.1016/j.dendro.2007.12.001

Melvin, T. M., Briffa, K. R., Nicolussi, K., & Grabner, M. (2007). Time-varying-response smoothing. *Dendrochronologia*, *25*(1), 65–69. https://doi.org/10.1016/j.dendro.2007.01.004

Mills, C. M., & Walsh, J. E. (2013). Seasonal variation and spatial patterns of the atmospheric component of the Pacific decadal oscillation. *Journal of Climate*, *26*(5), 1575–1594. https://doi.org/10.1175/JCLI-D-12-00264.1

Moodie, D. W., Catchpole, A. J. W., & Abel, K. (1992). Northern Athapaskan oral traditions and the white river volcano. *Ethnohistory*, *39*(2), 148. https://doi.org/10.2307/482391

Moreno-Chamarro, E., Zanchettin, D., Lohmann, K., & Jungclaus, J. H. (2015). Internally generated decadal cold events in the northern North Atlantic and their possible implications for the demise of the Norse settlements in Greenland: Cold events in subpolar North Atlantic. *Geophysical Research Letters*, *42*(3), 908–915. https://doi.org/10.1002/2014GL062741

Nash, D. J., Adamson, G. C. D., Ashcroft, L., Bauch, M., Camenisch, C., Degroot, D., et al. (2021). Climate indices in historical climate reconstructions: A global state of the art. *Climate of the Past*, *17*(3), 1273–1314. https://doi.org/10.5194/cp-17-1273-2021

NCAR. (2022). NP index data [Dataset]. Climate Analysis Section, NCAR. Retrieved from https://climatedataguide.ucar.edu/climate-data/north-pacific-np-index-trenberth-and-hurrell-monthly-and-winter

Newman, M., Alexander, M. A., Ault, T. R., Cobb, K. M., Deser, C., Di Lorenzo, E., et al. (2016). The Pacific decadal oscillation, revisited. *Journal of Climate*, *29*(12), 4399–4427. https://doi.org/10.1175/JCLI-D-15-0508.1

Oppenheimer, C. (2003). Climatic, environmental and human consequences of the largest known historic eruption: Tambora volcano (Indonesia) 1815. *Progress in Physical Geography: Earth and Environment*, *27*(2), 230–259. https://doi.org/10.1191/0309133303pp379ra

PAGES 2k Consortium. (2019). Consistent multidecadal variability in global temperature reconstructions and simulations over the Common Era. *Nature Geoscience*, *12*(8), 643–649. https://doi.org/10.1038/s41561-019-0400-0

Papineau, J. M. (2001). Wintertime temperature anomalies in Alaska correlated with ENSO and PDO. *International Journal of Climatology*, *21*(13), 1577–1592. https://doi.org/10.1002/joc.686

Raible, C. C., Brönnimann, S., Auchmann, R., Brohan, P., Frölicher, T. L., Graf, H., et al. (2016). Tambora 1815 as a test case for high impact volcanic eruptions: Earth system effects. *WIREs Climate Change*, *7*(4), 569–589. https://doi.org/10.1002/wcc.407

Rao, M. P., Cook, B. I., Cook, E. R., D'Arrigo, R. D., Krusic, P. J., Anchukaitis, K. J., et al. (2017). European and Mediterranean hydroclimate responses to tropical volcanic forcing over the last millennium. *Geophysical Research Letters*, *44*(10), 5104–5112. https://doi.org/10.1002/2017GL073057

R Core Team. (2021). R: A language and environment for statistical computing [Software]. R Foundation for Statistical Computing. Retrieved from https://www.R-project.org/

Reid, E., & Wilson, R. (2020). Delta blue intensity vs. maximum density: A case study using Pinus uncinata in the Pyrenees. *Dendrochronologia*, *61*, 125706. https://doi.org/10.1016/j.dendro.2020.125706

Robock, A. (2000). Volcanic eruptions and climate. *Reviews of Geophysics*, *38*(2), 191–219. https://doi.org/10.1029/1998RG000054

Salzer, M. W., & Hughes, M. K. (2007). Bristlecone pine tree rings and volcanic eruptions over the last 5000 yr. *Quaternary Research*, *67*(1), 57–68. https://doi.org/10.1016/j.yqres.2006.07.004

Schneider, L., Smerdon, J. E., Büntgen, U., Wilson, R. J. S., Myglan, V. S., Kirdyanov, A. V., & Esper, J. (2015). Revising midlatitude summer temperatures back to A.D. 600 based on a wood density network. *Geophysical Research Letters*, *42*(11), 4556–4562. https://doi.org/10.1002/2015GL063956

Schneider, L., Smerdon, J. E., Pretis, F., Hartl-Meier, C., & Esper, J. (2017). A new archive of large volcanic events over the past millennium derived from reconstructed summer temperatures. *Environmental Research Letters*, *12*(9), 094005. https://doi.org/10.1088/1748-9326/aa7a1b

Schweingruber, F. H., & Briffa, K. R. (1996). Tree-ring density networks for climate reconstruction. In *Climatic variations and forcing mechanisms of the last 2000 years* (pp. 43–66). Springer.

Stahle, D. W., & Dean, J. S. (2011). North American tree rings, climatic extremes, and social disasters. In M. K. Hughes, T. W. Swetnam, & H. F. Diaz (Eds.), *Dendroclimatology* (Vol. 11, pp. 297–327). Springer Netherlands. https://doi.org/10.1007/978-1-4020-5725-0_10

St. George, S. (2014). An overview of tree-ring width records across the Northern Hemisphere. *Quaternary Science Reviews*, *95*, 132–150. https://doi.org/10.1016/j.quascirev.2014.04.029

Stine, A. R., & Huybers, P. (2014). Arctic tree rings as recorders of variations in light availability. *Nature Communications*, *5*(1), 3836. https://doi.org/10.1038/ncomms4836

Stoffel, M., Khodri, M., Corona, C., Guillet, S., Poulain, V., Bekki, S., et al. (2015). Estimates of volcanic-induced cooling in the Northern Hemisphere over the past 1,500 years. *Nature Geoscience*, *8*(10), 784–788. https://doi.org/10.1038/ngeo2526

Tierney, J. E., Abram, N. J., Anchukaitis, K. J., Evans, M. N., Giry, C., Kilbourne, K. H., et al. (2015). Tropical sea surface temperatures for the past four centuries reconstructed from coral archives. *Paleoceanography*, *30*(3), 226–252. https://doi.org/10.1002/2014PA002717

Timmreck, C., Toohey, M., Zanchettin, D., Brönnimann, S., Lundstad, E., & Wilson, R. (2021). The unidentified eruption of 1809: A climatic cold case. *Climate of the Past*, *17*(4), 1455–1482. https://doi.org/10.5194/cp-17-1455-2021

Toohey, M., & Sigl, M. (2017). Volcanic stratospheric sulfur injections and aerosol optical depth from 500 BCE to 1900 CE. *Earth System Science Data*, *9*(2), 809–831. https://doi.org/10.5194/essd-9-809-2017

Trenberth, K. E., Branstator, G. W., Karoly, D., Kumar, A., Lau, N.-C., & Ropelewski, C. (1998). Progress during TOGA in understanding and modeling global teleconnections associated with tropical sea surface temperatures. *Journal of Geophysical Research*, *103*(C7), 14291–14324. https://doi.org/10.1029/97JC01444

Trenberth, K. E., & Hurrell, J. W. (1994). Decadal atmosphere-ocean variations in the Pacific. *Climate Dynamics*, *9*(6), 303–319. https://doi.org/10.1007/BF00204745

Trinies, C. A., Bunn, A. G., Robertson, C. S., & Anchukaitis, K. J. (2022). Dendroclimatology of Yellow-Cedar (Callitropsis nootkatensis) and temperature variability on the western slopes of the North Cascades in Washington State, USA, from 1333 to 2015 CE. *Tree-Ring Research*, *78*(2), 113–138. https://doi.org/10.3959/2021-20

Trouet, V., & Taylor, A. H. (2010). Multi-century variability in the Pacific North American circulation pattern reconstructed from tree rings. *Climate Dynamics*, *35*(6), 953–963. https://doi.org/10.1007/s00382-009-0605-9

Vargo, L. (2013). *Tree-ring evidence of North Pacific volcanically forced cooling and forcing of the Pacific Decadal Oscillation (PDO)* (Undergraduate Thesis). College of Wooster.

Vincent, L. A., Zhang, X., Brown, R. D., Feng, Y., Mekis, E., Milewska, E. J., et al. (2015). Observed trends in Canada's climate and influence of low-frequency variability modes. *Journal of Climate*, *28*(11), 4545–4560. https://doi.org/10.1175/JCLI-D-14-00697.1

Wang, T., Otterå, O. H., Gao, Y., & Wang, H. (2012). The response of the North Pacific Decadal Variability to strong tropical volcanic eruptions. *Climate Dynamics*, *39*(12), 2917–2936. https://doi.org/10.1007/s00382-012-1373-5

Wegmann, M., Brönnimann, S., Bhend, J., Franke, J., Folini, D., Wild, M., & Luterbacher, J. (2014). Volcanic influence on European summer precipitation through monsoons: Possible cause for "Years without Summer". *Journal of Climate*, *27*(10), 3683–3691. https://doi.org/10.1175/JCLI-D-13-00524.1

Wiles, G. C., D'Arrigo, R. D., Barclay, D., Wilson, R. S., Jarvis, S. K., Vargo, L., & Frank, D. (2014). Surface air temperature variability reconstructed with tree rings for the Gulf of Alaska over the past 1200 years. *The Holocene*, *24*(2), 198–208. https://doi.org/10.1177/0959683613516815

Wilson, R., Anchukaitis, K., Andreu-Hayles, L., Cook, E., D'Arrigo, R., Davi, N., et al. (2019a). Improved dendroclimatic calibration using blue intensity in the southern Yukon. *The Holocene*, *29*(11), 1817–1830. https://doi.org/10.1177/0959683619862037

Wilson, R., Anchukaitis, K., Andreu-Hayles, L., Cook, E., D'Arrigo, R., Davi, N., et al. (2019b). NOAA/WDS Paleoclimatology - Southwestern Yukon 668 Year Summer Temperature Reconstruction [Dataset]. NOAA National Centers for Environmental Information. https://doi.org/10.25921/qx61-9s04

Wilson, R., Anchukaitis, K., Briffa, K. R., Büntgen, U., Cook, E., D'Arrigo, R., et al. (2016a). Last millennium Northern Hemisphere summer temperatures from tree rings: Part I: The long term context. *Quaternary Science Reviews*, *134*, 1–18. https://doi.org/10.1016/j.quascirev.2015.12.005

Wilson, R., Anchukaitis, K., Briffa, K. R., Büntgen, U., Cook, E., D'Arrigo, R., et al. (2016b). NOAA/WDS Paleoclimatology - Northern Hemisphere 1250 year N-trend summer temperature reconstructions [Dataset]. NOAA National Centers for Environmental Information. https://doi.org/10.25921/kztr-jd59

Wilson, R., D'Arrigo, R., Andreu-Hayles, L., Oelkers, R., Wiles, G., Anchukaitis, K., & Davi, N. (2017). Experiments based on blue intensity for reconstructing North Pacific temperatures along the Gulf of Alaska. *Climate of the Past*, *13*(8), 1007–1022. https://doi.org/10.5194/cp-13-1007-2017

Wilson, R., D'Arrigo, R., Andreu-Hayles, L., Oelkers, R., Wiles, G., Anchukaitis, K., & Davi, N. (2023). NOAA/WDS Paleoclimatology - Gulf of Alaska air temperature reconstuction based on delta blue intensity of tree rings (1600–2010 CE) [Dataset]. NOAA National Centers for Environmental Information. Retrieved from https://www.ncei.noaa.gov/access/paleo-search/study/37638

Wilson, R., Rao, R., Rydval, M., Wood, C., Larsson, L.-Å., & Luckman, B. H. (2014). Blue intensity for dendroclimatology: The BC blues: A case study from British Columbia, Canada. *The Holocene*, *24*(11), 1428–1438. https://doi.org/10.1177/0959683614544051

Wilson, R., Rao, R., Rydval, M., Wood, C., Larsson, L.-Å., & Luckman, B. H. (2016). NOAA/WDS Paleoclimatology - Southern British Columbia 400 year summer temperature reconstructions [Dataset]. NOAA National Centers for Environmental Information. https://doi.org/10.25921/kxjd-vm75

Wilson, R., Tudhope, A., Brohan, P., Briffa, K., Osborn, T., & Tett, S. (2006). Two-hundred-fifty years of reconstructed and modeled tropical temperatures. *Journal of Geophysical Research*, *111*(C10), C10007. https://doi.org/10.1029/2005JC003188

Wise, E. K. (2015). Tropical Pacific and Northern Hemisphere influences on the coherence of Pacific Decadal Oscillation reconstructions: Climate influences on PDO inter-reconstruction coherence. *International Journal of Climatology*, *35*(1), 154–160. https://doi.org/10.1002/joc.3966

Woodhouse, C. A., Lukas, J. J., & Brown, P. M. (2002). Drought in the western Great Plains, 1845–56: Impacts and implications. *Bulletin of the American Meteorological Society*, *83*(10), 1485–1494. https://doi.org/10.1175/bams-83-10-1485

Yalcin, K., Wake, C. P., Kreutz, K. J., Germani, M. S., & Whitlow, S. I. (2006). Ice core evidence for a second volcanic eruption around 1809 in the Northern Hemisphere. *Geophysical Research Letters*, *33*(14), L14706. https://doi.org/10.1029/2006GL026013

Zanchettin, D. (2017). Aerosol and solar irradiance effects on decadal climate variability and Predictability. *Current Climate Change Reports*, *3*(2), 150–162. https://doi.org/10.1007/s40641-017-0065-y

Zanchettin, D., Bothe, O., Graf, H. F., Lorenz, S. J., Luterbacher, J., Timmreck, C., & Jungclaus, J. H. (2013). Background conditions influence the decadal climate response to strong volcanic eruptions: Volcanic forcing and background climate. *Journal of Geophysical Research: Atmospheres*, *118*(10), 4090–4106. https://doi.org/10.1002/jgrd.50229

Zanchettin, D., Bothe, O., Lehner, F., Ortega, P., Raible, C. C., & Swingedouw, D. (2015). Reconciling reconstructed and simulated features of the winter Pacific/North American pattern in the early 19th century. *Climate of the Past*, *11*(6), 939–958. https://doi.org/10.5194/cp-11-939-2015

Zanchettin, D., Rubino, A., Matei, D., Bothe, O., & Jungclaus, J. H. (2013). Multidecadal-to-centennial SST variability in the MPI-ESM simulation ensemble for the last millennium. *Climate Dynamics*, *40*(5–6), 1301–1318. https://doi.org/10.1007/s00382-012-1361-9

Zanchettin, D., Timmreck, C., Toohey, M., Jungclaus, J. H., Bittner, M., Lorenz, S. J., & Rubino, A. (2019). Clarifying the relative role of forcing uncertainties and initial-condition unknowns in spreading the climate response to volcanic eruptions. *Geophysical Research Letters*, *46*(3), 1602–1611. https://doi.org/10.1029/2018GL081018